An update to this article is included at the end

EBioMedicine 59 (2020) 102912

Contents lists available at ScienceDirect

EBioMedicine

journal homepage: www.elsevier.com/locate/ebiom

Research paper

Obesity-related hypoxia via miR-128 decreases insulin-receptor expression in human and mouse adipose tissue promoting systemic insulin resistance

Biagio Arcidiacono[a], Eusebio Chiefari[a], Anna Foryst-Ludwig[b], Giuseppe Currò[a], Giuseppe Navarra[c], Francesco S. Brunetti[a], Maria Mirabelli[a], Domenica M. Corigliano[a], Ulrich Kintscher[b], Domenico Britti[a], Vincenzo Mollace[a], Daniela P. Foti[a], Ira D. Goldfine[d], Antonio Brunetti[a,*]

[a] Department of Health Sciences, University of Catanzaro "Magna Græcia", Viale Europa, 88100 Catanzaro, Italy
[b] Institute of Pharmacology, Center for Cardiovascular Research, Charité Universitätsmedizin, 10115 Berlin, Germany
[c] Department of Human Pathology of Adult and Evolutive Age, University Hospital of Messina, 98122 Messina, Italy
[d] Department of Medicine, University of California San Francisco, 94143 San Francisco, USA

ARTICLE INFO

Article History:
Received 1 May 2020
Revised 5 July 2020
Accepted 8 July 2020
Available online 29 July 2020

Keywords:
Obesity
Adipose-tissue dysfunction
Hypoxia
Insulin receptor
Insulin resistance
miRNA
mRNA decay

ABSTRACT

Background: Insulin resistance in visceral adipose tissue (VAT), skeletal muscle and liver is a prominent feature of most patients with obesity. How this association arises remains poorly understood. The objective of this study was to demonstrate that the decrease in insulin receptor (INSR) expression and insulin signaling in VAT from obese individuals is an early molecular manifestation that might play a crucial role in the cascade of events leading to systemic insulin resistance.
Methods: To clarify the role of INSR and insulin signaling in adipose tissue dysfunction in obesity, we first measured INSR expression in VAT samples from normal-weight subjects and patients with different degrees of obesity. We complemented these studies with experiments on high-fat diet (HFD)-induced obese mice, and in human and murine adipocyte cultures, in both normoxic and hypoxic conditions.
Findings: An inverse correlation was observed between increasing body mass index and decreasing INSR expression in VAT of obese humans. Our results indicate that VAT-specific downregulation of INSR is an early event in obesity-related adipose cell dysfunction, which increases systemic insulin resistance in both obese humans and mice. We also provide evidence that obesity-related hypoxia in VAT plays a determinant role in this scenario by decreasing INSR mRNA stability. This decreased stability is through the activation of a miRNA (miR-128) that downregulates INSR expression in adipocytes.
Interpretation: We present a novel pathogenic mechanism of reduced INSR expression and insulin signaling in adipocytes. Our data provide a new explanation linking obesity with systemic insulin resistance.
Funding: This work was partly supported by a grant from Nutramed (PON 03PE000_78_1) and by the European Commission (FESR FSE 2014-2020 and Regione Calabria).
© 2020 The Author(s). Published by Elsevier B.V. This is an open access article under the CC BY-NC-ND license. (http://creativecommons.org/licenses/by-nc-nd/4.0/)

1. Introduction

Obesity affects over 30% of the world's population [1]. Obesity is the most common cause of insulin resistance, where the classical insulin target tissues, fat, muscle, and liver fail to respond normally to circulating insulin [2]. Insulin resistance is a major risk factor for the development of type 2 diabetes (T2D) mellitus, and cardiovascular diseases [3]. How adiposity influences insulin resistance in the major insulin sensitive tissues remains unknown.

Visceral adipose tissue (VAT) has emerged as a major endocrine organ, producing a variety of adipocytokines and other factors that affect lipid metabolism and glucose homeostasis, and may increase cardiovascular risk, as well as thrombotic and inflammatory pathways, and signaling networks in cancer [4–6]. The contribution of VAT inflammation to the development of obesity-related systemic insulin resistance has been well documented [7–10], although the exact role that VAT plays in the pathogenesis of insulin resistance is

* Corresponding author.
E-mail address: brunetti@unicz.it (A. Brunetti).

https://doi.org/10.1016/j.ebiom.2020.102912
2352-3964/© 2020 The Author(s). Published by Elsevier B.V. This is an open access article under the CC BY-NC-ND license. (http://creativecommons.org/licenses/by-nc-nd/4.0/)

Research in context

Evidence before this study

Obesity is a major cause of insulin resistance. Evidence indicates that progressive visceral adipose tissue (VAT) accumulation in obesity leads to local hypoxia. This hypoxia promotes a generalized change in the circulating levels of adipocytokines and other factors that adversely affect insulin signaling, leading to systemic insulin resistance. The causal relationship between VAT accumulation and a decreased expression of the insulin receptor (INSR) in VAT remains unknown. Thus, the mechanism of VAT-induced insulin resistance needs to be established.

Added value of this study

We have now analyzed VAT samples from patients with increasing levels of body mass index (BMI). Our analysis indicates that INSR expression in VAT correlates inversely with increasing BMI. Similar results were obtained with diet-induced obese mice. Downregulation of the INSR was also observed in cultures of isolated human visceral adipocytes from normal-weight subjects when incubated under low oxygen tension. This observation suggests that obesity-related hypoxia in VAT plays a role in INSR downregulation. Hypoxia-induced downregulation of INSR in cultured adipocytes was reversed by restoration of the oxygen supply, supporting the dependence of INSR expression on the oxygen concentration in the cellular environment. Moreover we now find that reduced INSR expression by hypoxia is mediated via activation of the unique miRNA (miR-128). miR-128 downregulates the INSR in adipocytes by affecting INSR mRNA stability. We hypothesize that miR-128 may contribute to systemic insulin resistance via INSR downregulation, and also the release of adipose-derived adipokines and proinflammatory molecules that adversely affect peripheral insulin action.

Implications of all the available evidence

Our findings demonstrate a newly defined pathogenic mechanism of reduced INSR expression and insulin signaling in visceral adipocytes from obese individuals, and provide a new explanation linking obesity with systemic insulin resistance. Therefore, targeted inhibition of miR-128 in adipose tissue may constitute a new strategy to ameliorate insulin resistance in obesity.

unknown. The systemic inflammatory response of obesity can lead to the activation of stress kinases in VAT, such as the inhibitor of nuclear factor-kB kinase, IKK, and the c-Jun N-terminal kinase 1, JNK1, both of which impair insulin action via phosphorylation of the insulin receptor (INSR) substrate 1 (IRS1) on inhibitory serine residues instead of stimulatory tyrosine residues, thus blocking downstream INSR signaling [11].

The role of adipose tissue in promoting systemic insulin resistance was initially supported by studies indicating that the insulin-sensitive muscle/fat glucose transporter, GLUT4, is downregulated in adipose tissue, but not in skeletal muscle of humans and rodents with obesity and T2D [12]. Also, studies in the last decades have greatly implemented our understanding of the biological role of adipose tissue in the regulation of glucose homeostasis and energy balance, by demonstrating that this tissue produces a variety of bioactive molecules, collectively known as adipocytokines, such as tumor necrosis factor α (TNF-α) and interleukin 6 (IL-6), the abnormal expression of which has been strongly associated with inflammation, insulin resistance and type 2 diabetes [13,14]. On the other hand, a striking relationship between overaccumulation of fat in skeletal muscle with insulin sensitivity occurs early during the natural course of obesity [15,16]. Furthermore, recent studies have also revealed that microRNAs (miRNAs) produced by adipose tissue may induce insulin resistance and glucose intolerance in mouse models of obesity [17–19].

The hormone insulin exerts its biological effects by binding to the INSR, a plasma membrane tyrosine kinase receptor protein. When insulin binds to the INSR, it induces intracellular events leading to the cellular response to insulin [20–22]. Therefore, the role of INSR has been widely investigated in the pathogenesis of insulin resistance. However, its role in the development of obesity-related insulin resistance is unclear [23–25]. Previously, it has been reported that fat-specific INSR-deficient mice show severe lipodystrophy, hyperinsulinemic diabetes, hyperlipidemia and fatty liver disease [26,27]. Recently, the significance of adipocyte INSR expression in the development of systemic insulin resistance has been supported by the identification of specific miRNAs, such as miR-27b, which are upregulated both in in vitro and in in vivo models of insulin resistance, and suppress adipocyte INSR expression by targeting INSR 3′-UTR directly [28].

On the basis of these considerations, we aimed to investigate the involvement of INSR in the pathogenesis of obesity-associated insulin resistance in the major insulin sensitive tissues. We hypothesized that hypoxia, a well-established characteristic of obese adipose tissue, could play a role on the expression of INSR in VAT. Through a series of in vitro and in vivo molecular studies in humans and mice, combined with measurements of obesity-related metabolic and inflammatory biomarkers in humans, we now provide evidence that an inverse correlation exists between increasing body mass index (BMI) and decreasing INSR in human VAT during the progression from mild to severe and very severe obesity. Moreover, we present a novel pathogenic mechanism of reduced INSR mRNA and protein expression in adipocytes, which may also provide an explanation linking obesity with systemic insulin resistance.

2. Materials and methods

2.1. Patients

Omental VAT specimens from 26 consecutive, unrelated, obese subjects, were collected during elective bariatric surgery. Obesity was defined as body mass index (BMI) $\geq$ 30 kg/m^2 based on the World Health Organization criteria [29]. The main clinical features and biochemical characteristics of patients before surgical intervention are in Table 1. Fasting blood samples were collected and biochemical analyses of plasma glucose and serum insulin levels were carried out by standard methods in all subjects who had no caloric intake for at least 8 h. Insulin resistance was calculated with the homeostatic model assessment method of insulin resistance (HOMA-IR) [30]. Serum samples were frozen in aliquots for subsequent analyses, including adiponectin and resistin by ELISA methods [5], RBP-4 and hs-CRP by nephelometric methods on a BNII analyzer (Siemens), and cytokines and VEGF using a protein biochip array technology (Randox Labs) [31]. Criteria for exclusion of patients from this study were: secondary obesity, genetic syndromes of insulin resistance, type 1 or T2D, previous gestational diabetes mellitus, hepatic or renal impairment, presence of malignancies or rheumatologic disease, treatment with medications affecting glucose tolerance.

Omental VAT was also collected from the abdomen of 20 normal weight (BMI 18.5–24.9 kg/m^2) metabolically healthy subjects, that underwent open abdominal surgery. A portion of each specimen was immediately snap-frozen in liquid nitrogen and stored at −80 °C until protein and RNA extraction. The protocol was approved by the Ethics Committee of the University of Messina, Italy (approval no: 489 of

Table 1
Clinical and biochemical features of enrolled subjects.

	Controls BMI 18.5–24.9 A	Group 1 BMI 30–34.9 B	Group 2 BMI 35–39.9 C	Group 3 BMI ≥ 40 D	*p*
Number, *n*	20	7	8	11	–
Ethnicity	Caucasian	Caucasian	Caucasian	Caucasian	–
Female, *n*	13 (65.0%)	4 (57.1%)	4 (50%)	9 (81.8%)	ns
Age, yr	67.7 ± 5.9	51.9 ± 5.1	52.7 ± 9.5	41.8 ± 8.5	< 0.001
BMI, kg/m^2	23.6 ± 1.5	32.1 ± 1.2	37.2 ± 1.7	45.8 ± 6.1	< 0.001
Hypertension, *n*	0	5 (71.4%)	8 (100%)	11 (100%)	< 0.001 (A vs B) < 0.001 (A vs C) < 0.001 (A vs D)
Dyslipidemia, *n*	0	6 (85.7%)	8 (100%)	11 (100%)	< 0.001 (A vs B) < 0.001 (A vs C) < 0.001 (A vs D)
FPG, mg/dL	87.5 ± 7.2	99.6 ± 10.2	101.9 ± 11.0	97.3 ± 11.0	0.003
IFG, *n*	0	2	3	5	0.017 (A vs C) 0.003 (A vs D)
Insulin, μU/mL	4.6 ± 2.0	14.9 ± 2.7	16.1 ± 4.0	25.7 ± 10.4	< 0.001
HOMA-IR	1.0 ± 0.5	3.6 ± 0.5	4.1 ± 1.2	6.4 ± 3.2	< 0.001

Data are mean ± SD or number (*n*). Kruskall–Wallis test was employed for continuous values comparisons. Fisher's exact test was used for comparison of categorical trait. In this latter case, only significant comparisons are shown. BMI, body mass index; FPG, fasting plasma glucose; IFG, impaired fasting glucose; HOMA-IR, homeostatic model assessment method of insulin resistance.

April 7, 2016), and the study performed in accordance with the Declaration of Helsinki. All subjects gave written informed consent.

2.2. Organ culture and isolated human adipocytes

A portion of VAT from non-obese/metabolically healthy subjects was used for organ culture experiments. To this end, adipose tissue specimens (~250 mg/60 mm dishes) were minced into small pieces (2 mm^3) using sterile scissors, cultured in serum free medium 199 (Gibco), and incubated at 37 °C in 5% CO_2. To mimic the in vivo conditions [9], adipose tissue organ control cultures were incubated in 7% O_2, while the hypoxic condition was set as 1% O_2. Then, the adipose tissue cultures were ready to be used for next experiments. Isolated human adipocytes were prepared as described previously [32]. In brief, biopsies of VAT were placed into 50 mL tube containing 1 mg/mL collagenase (type 1) solution, and incubated in a 37 °C water bath for 1 h. At the end of incubation, the digested mixture was filtered through a nylon mesh filter, and the filtrate washed three times with medium 199. Isolated adipocytes were separated from the stromal vascular fraction after centrifuging at 500 g for 1 min and immediately used for experiments under normoxic or hypoxic conditions.

2.3. mRNA extraction, real-time PCR and miRNA expression profile

Total RNA from ~300 mg of adipose tissue was isolated using 1 mL of TRIzol reagent (Life Technologies), following the manufacturer's recommended protocol, and quantified with a NanoDrop Spectrophotometer (Thermo Fisher Scientific). RNA levels were normalized against 18 S ribosomal RNA in each sample, and cDNAs were synthesized from 1 μg of total RNA, using High Capacity cDNA Reverse Transcription Kit (Applied Biosystems). For miRNA experiments, RNA levels were normalized to that of miRNA-U6 as internal control and cDNA were synthesized from 50 ng of total RNA using the TaqMan MicroRNA Reverse Transcription kit (Thermo Fisher Scientific). Sequence-specific primers for human and mouse INSR, PEPCK and ribosomal protein S9 (RPS9), designed according to sequences from the GenBank database, are listed in Supplementary Table S1. In particular, with respect to the two isoforms (A and B) of the INSR, primers specifically targeted shared sequences of the INSR. Green fluorescence was measured, and relative quantification was made against the RPS9 cDNA used as an internal standard. All PCR reactions were carried out in triplicates. A custom TaqMan Array Human MicroRNA plate (Applied Biosystems) was used to measure miRNA expression profile in hypoxic and normoxic 3T3-L1 cells. The panel contained 96 miRNAs that were previously found to be involved in human adipose tissue and obesity [33–35]. The miRNA expression levels were normalized to RNU48 and relative expression values were obtained using the relative quantification RQ=$2^{\Delta\Delta ct}$. miRNAs whose mean RQ levels were < 0.5 (downexpressed) or > 2 (upexpressed) in hypoxic vs normoxic 3T3-L1 cells were considered differentially expressed.

2.4. Western blot (WB)

~1 g of adipose tissue was used to prepare cytoplasmic and nuclear protein extracts, as previously described [36]. All WB experiments were performed following standard procedures, using the following primary antibodies: anti-INSR polyclonal antibody (Insulin Rβ - C-19, 1:500; Santa Cruz Biotechnology), recognizing both A and B isoforms of INSR; anti-IRS1 (2390S, 1:1000; Cell Signaling); anti-pIRS1 (Tyr896, 44–818 G; ThermoFisher); anti-Akt (4685, 1:1000; Cell Signaling); anti-phospho-Akt Ser^{473} and Thr^{308} (9271S, 9275S, 1:1000; Cell Signaling); anti IGF-IR (9750, 1:1000; Cell Signaling), anti-GLUT4 polyclonal antibody [37]; anti-HIF-1α polyclonal antibody (NB 100–134, Novus Biologicals); anti-VEGFA specific antibody (A-20 - sc152, Santa Cruz Biotechnology); anti-β actin (clone AC-15, A5441 Sigma Aldrich).

2.5. Animals and diet-induced obesity (DIO) model

Twenty 5-week-old male C57BL/6 J mice were housed in a temperature-controlled facility (25 °C) with a 12 h light-dark cycle. Following previous indications [38], a group of 10 mice were fed ad libitum with high fat diet (HFD): 60% kcal from fat, 20% kcal from carbohydrates, 20% kcal from protein, for 15 weeks. A second group of 10 mice (control group) were fed with normal chow diet (NCD): 10% kcal from fat, 70% kcal from carbohydrates, 20% kcal from protein, for 15 weeks. At the end of the 15-week period, mice were sacrificed by cervical dislocation and liver, quadriceps muscle, and intra-abdominal visceral fat were removed and immediately frozen in liquid nitrogen.

Insulin tolerance tests (ITT) were performed in both HFD and NCD groups, by measuring blood glucose levels in 12 h fasted conscious mice injected intraperitoneally with human insulin (Human Actrapid,

Novo Nordisk), 1 U/kg body weight) [39]. Blood was collected from the orbital sinus, and glucose levels were measured at the indicated times, before and after injection, using the Glucocard glucometer (Menarini Diagnostics). For other biochemical analyses, blood samples were collected after 12 h of fasting, and serum samples were stored at −20 °C. Insulin was measured using an ultrasensitive rat/mouse insulin ELISA kit (EMD Millipore Corporation). All animal work was performed using approved animal protocols, in accordance with institutional guidelines for the care of laboratory animals (directive 86/609/ECC, European Community Council).

2.6. Cell cultures and cell differentiation

Human embryonic kidney 293 (HEK-293) cells were cultured in Dulbecco's modified Eagle medium (DMEM), supplemented with 10% fetal bovine serum (FBS) (Gibco Laboratories), 2 mM glutamine, penicillin (100 U/mL) and streptomycin (100 μg/mL), in a humidified 5% CO_2 atmosphere at 37 °C. Mouse 3T3-L1 fibroblasts were differentiated into 3T3-L1 adipocytes as described previously [40,41]. Briefly, confluent 3T3-L1 cells in DMEM-10% FBS on 6-well plates were induced to differentiate in complete medium containing 1 μM dexamethasone, 500 μM 3-isobutyl-1-methyxanthine and 1 μg/mL insulin for three days. Afterward, cells were incubated in DMEM containing 10% FBS and 1 μg/mL insulin for two days. After day 5, cells were then maintained in DMEM-10% FBS, changing medium every two days. Experiments were performed using day 8 to day 12 mature 3T3-L1 adipocytes.

2.7. Hypoxia-induced insulin resistance and glucose uptake

Cells were cultured in serum free DMEM containing 0.5% bovine serum albumin (BSA), and incubated in the hypoxic glove chamber with 1% O_2/5% CO_2, at 37 °C for 48 h [42]. At the end of incubation, the chamber was opened in the anaerobic glove box (flushed with N2) to avoid reoxygenation and cells were used for successive experiments. To evaluate the absence of cytotoxicity after exposure to hypoxia, cell viability was tested by 3-(4,5-dimethythiazol-2-yl)−2,5-diphenyl tetrazolium bromide (MTT) assay, as described previously [43]. Control cells were incubated under the same experimental conditions except for the difference of the amount of used O_2 (7%). Glucose uptake in fully differentiated 3T3-L1 adipocytes was performed as described [44]. Briefly, cells were grown to confluence in 16-mm multiwell plates, either in normoxia or hypoxia, stimulated with 100 nM insulin (Sigma) in KRH [Na_2HPO_4 (0.01 M), NaCl (0.13 M), KCl (0.05 M), $MgSO_4 \bullet 7H_2O$ (0.0013 M), HEPES (0.0235 M) and $CaCl_2$ (0.0017 M)] containing 0.1% BSA buffer for 10 min, and incubated with 0.25 μCi of [^{3}H]2-deoxyglucose for 5 min. Cells were harvested in 0.05% SDS, and the uptake of [^{3}H]2-deoxyglucose measured by liquid scintillation counting. Non-specific glucose uptake was determined by using Cytochalasin-B and subtracted from the stimulated total glucose uptake.

2.8. Reporter gene assay, mRNA decay and miRNA transfection studies

For the luciferase (Luc) reporter gene assay, 3T3-L1 adipocytes were plated in 12-well plates (0.7×10^5 cells/well) and cultured for 24 h prior to transfection in DMEM supplemented with 10% FBS without antibiotics. Recombinant Luc reporter construct, pGL3-INSR-Luc (300 ng), containing the mouse *Insr* gene promoter (−1972/+2) was transiently transfected into cells, using the Lipofectamine 3000 reagent (Invitrogen). Twenty-four hours after transfection, cells were incubated at 37 °C, 1% O_2, 5% CO_2, while control cells were kept in normoxia (7% O_2). Luc activity was measured 24 h later in a luminometer (Tuner Biosystems), using the dual-luciferase reporter assay system (Promega). For the half-life and mRNA decay of INSR mRNA, 3T3-L1 adipocytes, treated or untreated with hypoxia, were exposed to 0.5−2.0 μg/mL of actinomycin D. RNA was extracted at 3-h intervals, cDNA was prepared and INSR mRNA levels were measured by real-time quantitative PCR (RT-qPCR), using RPS9 mRNA as control. Fifteen to 100 nM miR-128 mimic/inhibitor and its negative control (mirVana miRNA mimics Assay ID - MC11746 - Applied Biosystem) were transfected into 3T3-L1 adipocytes and HEK-293 cells, using the Lipofectamine RNAiMAX reagent (Invitrogen) for 48−72 h. Cells were, then, harvested and RNA and protein extracted for RT-qPCR and WB analysis, respectively.

2.9. Statistical analysis

Initially, continuous variables have been tested for normality of distribution using Shapiro−Wilk normal distribution test. Either the Student's *t*-test or the non-parametric Mann−Whitney test was used for comparisons of continuous variables between two groups, respectively, with normal and non-normal distribution. To compare continuous variables between four groups, the mean rank of each group with the mean rank of every other group was compared by the Kruskall−Wallis test, followed by the Dunn's test correction for multiple comparisons. The 2-tailed Fisher exact test was used for comparisons of proportions. A significance level of $P < 0.05$ was set for a type I error in all analyses. Bar graph data shown are the mean ± standard error of the mean (s.e.m.). All data were analyzed with Graphpad Prism 7.0 software (GraphPad Software).

3. Results

3.1. Characterization of enrolled subjects

Table 1 summarizes the main characteristics of the non-diabetic subjects enrolled in this study. Based on each patient's BMI (kg/m^2), they were divided into four groups: subjects with BMI 18.5−24.9 (controls); subjects with BMI 30.0−34.9 (group 1); subjects with BMI 35.0−39.9 (group 2); and subjects with BMI 40 and over (group 3). Multiple comparison analyses with post-hoc correction indicated that significant differences for all continuous variables existed among groups. In comparison with their normal-weight counterparts, all obese individuals were insulin resistant, as indicated by a HOMA-IR > 2.5, and they had hypertension, as defined by the 2017 ACC/AHA [45] and JNC7 [46] guidelines. Impaired fasting glucose was defined according to the American Diabetes Association (ADA) criteria [47]. None had overt diabetes. Dyslipidemia was defined according to ATP III of the National Cholesterol Education Program [48].

3.2. Downregulation of INSR in VAT of obese individuals

In an attempt to clarify the role of INSR in the pathophysiology of adipose tissue dysfunction in obesity, we first measured INSR expression in VAT from human samples. As measured by RT-qPCR and WB analyses, both INSR mRNA levels and protein expression were significantly reduced in VAT in obese subjects when compared to normal-weight control subjects (Fig. 1a). This reduction paralleled the progressive increase in BMI, with an almost complete loss of expression in the adipose tissue specimens obtained from patients in the BMI ≥ 40 group. As measured by RT-qPCR and WB, adipose-tissue expression of the closely related insulin-like growth factor I receptor (IGF-IR) was similar in all patient groups (Fig. 1b). This finding indicated that the observed reduction was specific for the INSR, and not the result of a nonspecific downregulation of gene expression.

The progressive reduction of INSR expression in VAT of obese individuals paralleled the decrease of IRS1 mRNA and protein expression levels and IRS1 serine phosphorylation levels (Fig. 1c). Degradation of IRS1 during hypoxia has been previously linked to caspase 3-mediated cleavage [49], as well as to chronic exposure to high insulin/glucose concentrations [50]. Noteworthy, in this regard, the

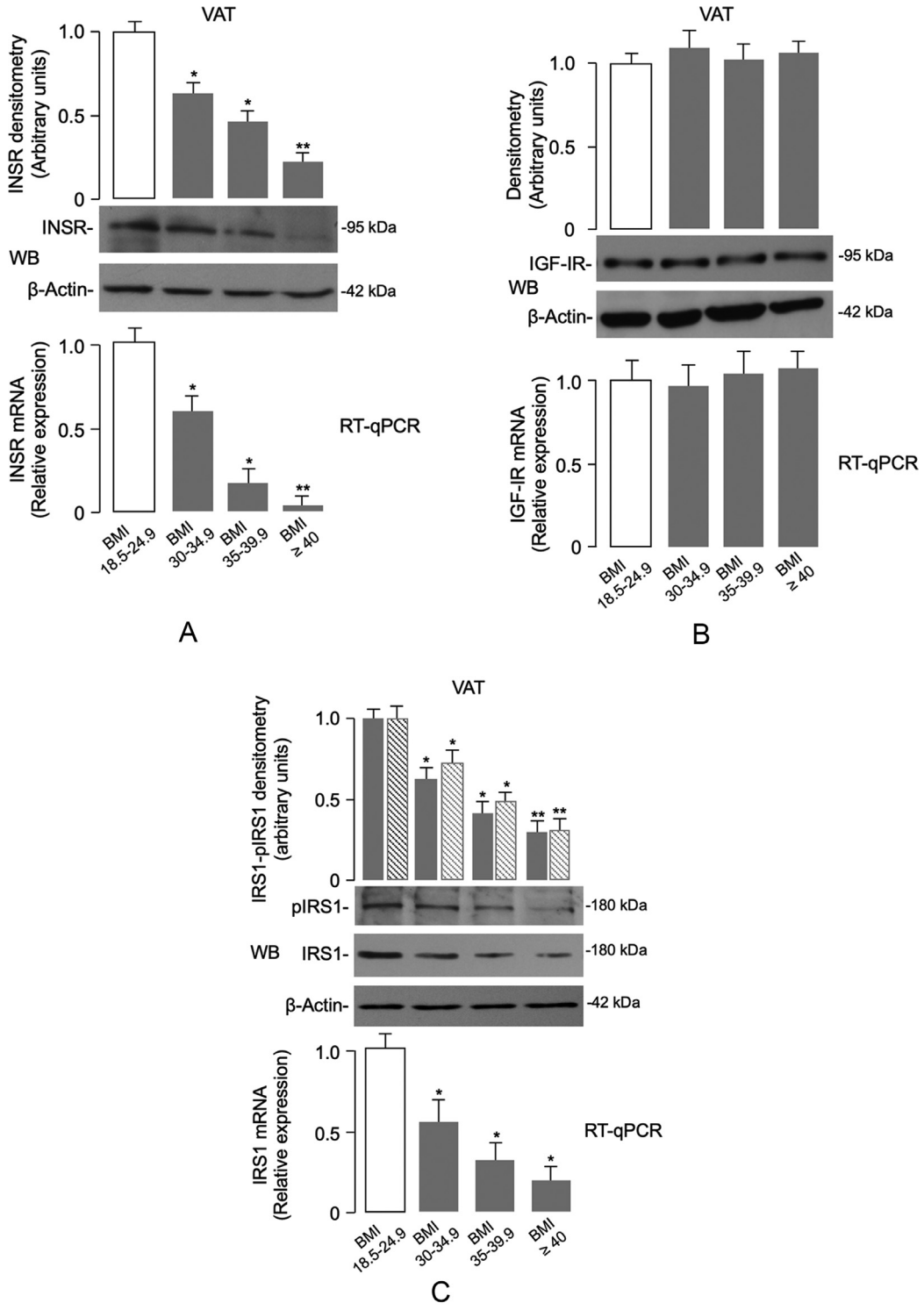

Fig. 1. INSR, IGF-IR and IRS1 expression in human VAT. (**A**) INSR mRNA and protein levels from the normal-weight and obese individuals were measured by real-time quantitative PCR (RT-qPCR) and Western blot (WB), respectively. The pattern of INSR mRNA and protein expression is shown in VAT samples from subjects in each BMI category (BMI 18.5−24.9 = 20 normal-weight subjects; BMI 30−34.9 = 7 obese subjects; BMI 35−39.9 = 8 obese subjects; BMI ≥ 40 = 11 obese subjects). A representative WB is shown. β-actin was employed as a control of protein loading. Densitometric scanning of INSR protein signals are shown in bar graphs. Levels of mRNA were normalized to RPS9 mRNA. Results are shown as mean ± s.e.m. $^{*}P < 0.05$ *vs* normal-weight subjects; $^{**}P < 0.05$ vs normal-weight subjects and vs individuals with BMI 30−34.9 [Student's *t*-test]. (**B**) IGF-IR mRNA and protein levels were measured as in (A), in VAT from normal-weight subjects and obese individuals. Bars represent the means of RT-qPCR and densitometric analysis of WB results from individuals in each BMI category. (**C**) Quantification of IRS1 mRNA and protein in VAT samples from subjects in each BMI category was as in (A). Densitometric scanning of total IRS1 (gray bars) and phosphorylated IRS1 (dashed bars) bands from representative WBs is shown. $^{*}P < 0.05$ vs normal-weight subjects; $^{**}P < 0.05$ vs normal-weight subjects and vs individuals with BMI 30−34.9 [Student's *t*-test].

inverse relationship between INSR/IRS-1 levels and the increasing trend in FPG, insulin and HOMA-IR across the different stages of obesity (Table 1), indicating that a functional link between INSR expression and insulin signaling during VAT accumulation and these metabolic parameters may exist.

3.3. INSR expression in hypoxic human adipocytes

Adipose tissue hypoxia is considered an important trigger of adipose cell dysfunction in both animal models and humans with obesity [9,51–53]. In this context, transgenic animal models constitutively overexpressing the hypoxia-inducible factor (HIF-1α) have importantly contributed to the definition of hypoxia-mediated effects on proteins and molecules involved in obesity-related insulin resistance [52,54,55]. As a step toward understanding the molecular mechanisms underlying the negative effects of human obesity on INSR production in fat, we first investigated the existence of a hypoxic condition in VAT of obese subjects. For this purpose, we measured the levels of HIF-1α, as well as the levels of the vascular endothelial growth factor A (VEGFA), a known target gene for HIF-1α, whose expression is triggered by hypoxia [40]. As shown in Fig. 2a, the protein abundance of both HIF-1α and VEGFA was increased in fat biopsies of VAT obtained from obese patients compared to those of normal-weight controls. The increased expression of HIF-1α and VEGFA in visceral fat closely correlated with the severity of adiposity, thereby indicating that a hypoxic response was occurring in adipose tissue during the progression of obesity.

In order to test the possibility of whether hypoxia could also affect INSR expression in VAT, we first carried out preliminary experiments using VAT from 12 normal-weight control subjects. VAT was placed in organ culture, either in normoxic or hypoxic conditions for 48 h. As shown in Fig. 2b, HIF-1α and VEGFA protein levels were respectively 5-fold and 2.5-fold greater in the hypoxic VAT fragments than in the normoxic fragments. Interestingly, restoration of oxygenation (reoxygenation) of adipose tissue fragments following hypoxic treatment restored the expression of both hypoxic markers (Fig. 2b), thus demonstrating the role of the hypoxic environment. To assess whether the source of HIF-1α and VEGFA under these conditions was the fat cell, similar measurements were determined in collagenase-isolated adipocytes obtained from samples of VAT from the same control subjects. HIF-1α and VEGFA protein expression from isolated visceral adipocytes in hypoxic conditions was significantly greater than that from normoxia-treated cells (Fig. 2c). Once again, reoxygenation of adipocytes after hypoxia restored the basal expression of both hypoxic markers (Fig. 2c), thus indicating that adipocytes themselves efficiently contribute to HIF-1α and VEGFA protein production.

Therefore, the expression of INSR was assessed in organ cultures of VAT, as well as in isolated visceral adipocytes from normal-weight control subjects, either in normoxia (7% O_2) or hypoxia (1% O_2). As shown in Fig. 2d, INSR mRNA levels and protein abundance were significantly reduced in adipose tissue fragments and isolated fat cells prepared from visceral fat depots when cultured in low oxygen tension. In concert with the above findings, subsequent reoxygenation for 24 h of either tissue or cells exposed to hypoxia enhanced INSR mRNA abundance and restored INSR protein expression (Fig. 2d). Of note, WB experiments revealed the presence of IGF-IR in organ culture but not in isolated adipocytes (data not shown). This finding indicated that the IGF-IR in fat was located in the stromovascular fraction, and this was consistent with previous observations using epididymal fat pads from HFD mice [56]. Reduced INSR expression in hypoxic adipose organ culture tissue and isolated human adipocytes paralleled the decrease in both IRS1 mRNA levels (Fig. 2d) and insulin-stimulated protein kinase B (Akt) phosphorylation in tissues and cells under hypoxic conditions (Fig. 2e), indicating therefore that hypoxia can induce downregulation of INSR expression and insulin signaling in human visceral fat in culture conditions, and that this effect can be reversed by restoration of oxygen supply. Consistently with these findings, translocation of the insulin-sensitive glucose transporter Glut4 protein to the plasma membrane was considerably decreased in hypoxic adipose tissue fragments and isolated adipocytes, and this reduction was reversed by reoxygenation (Fig. 2e). Restoration of INSR expression and signaling in human organ culture following reestablishment of oxygen tension indicates that obesity-related VAT dysfunction is not permanent and can be reversed.

3.4. Studies in a high-fat diet (HFD)-induced animal model of obesity

To further investigate the role of obesity-related hypoxia on INSR expression and insulin signaling, we next carried out in vivo studies using the HFD-induced obese (DIO) mouse. This animal model has proven to be a valuable model that accurately mimics common human obesity, with VAT accumulation, glucose intolerance, and hyperinsulinemia [38,42]. Twenty five-week-old male C57BL/6 J mice were randomized into two groups (n = 10/group). They were fed either with normal chow diet (NCD) or HFD for a period of 15 weeks, after which HFD-treated mice had maximum weight gain (~51 g), while there was a much lower weight gain (28 g) in control group (Supplementary Table S2). As expected, fasting plasma glucose and serum insulin levels in HFD mice were significantly higher than those in NCD mice (Supplementary Table S2), which were consistent with a condition of impaired fasting glucose and insulin resistance. In accordance with the recognized association between insulin resistance and lipid dysmetabolism [57], triglycerides and total cholesterol were significantly increased in mice fed with HFD, compared with mice subjected to NCD feeding (Supplementary Table S2), thereby confirming the validity of the DIO mouse model of human obesity. Consistent with the condition of peripheral insulin resistance, the glucose-lowering effect of exogenous insulin was reduced in HFD-treated mice during ITT (Fig. 3a). This result was substantiated at the molecular level by RT-qPCR data and immunoblot analyses, which showed that basal hepatic mRNA levels of phosphoenolpyruvate carboxykinase (Pepck), a gluconeogenic enzyme that is normally inhibited by insulin, were abnormally increased in HFD mice, whereas translocation of Glut4 protein to the plasma membrane, normally induced by insulin, was abnormally reduced in skeletal muscle from HFD-treated mice (Fig. 3b).

We then evaluated the expression of INSR in adipose tissue of DIO mice and controls. As measured by RT-qPCR and WB analysis, INSR mRNA levels and protein abundance were significantly reduced in VAT from DIO mice compared to those from control mice fed a NCD (Fig. 3c). Hypoxia in VAT from the HFD mouse model was confirmed by the rise in both HIF-1α and VEGFA levels (Fig. 3d). However, the mRNA levels of INSR did not differ significantly in both liver and skeletal muscle tissues between the two experimental animal groups (Fig. 3e), further supporting previous research that indicated a direct role of adipocyte and adipose tissue dysfunction in the pathogenesis of systemic insulin resistance [37,58–60].

3.5. Studies in 3T3-L1 cells

To further understand the dynamic changes affecting INSR expression during hypoxia as a paradigm of the obese state, we next determined the content of INSR in fully differentiated murine 3T3-L1 adipocytes, a cell model widely used for studying obesity-related characteristics, including insulin resistance [61]. In order to replicate a condition similar to that observed in humans and mice, hypoxia was induced in 3T3-L1 adipocytes [41,55]. The cellular expression of the INSR and insulin signaling activity were quantified thereafter. To verify the appropriateness of the experimental conditions, hypoxia in 3T3-L1 adipocytes was first confirmed by the increase of HIF-1α protein levels, then by increased expression of VEGFA (Fig. 4a). As shown in Fig. 4b, a significant reduction in INSR mRNA expression was

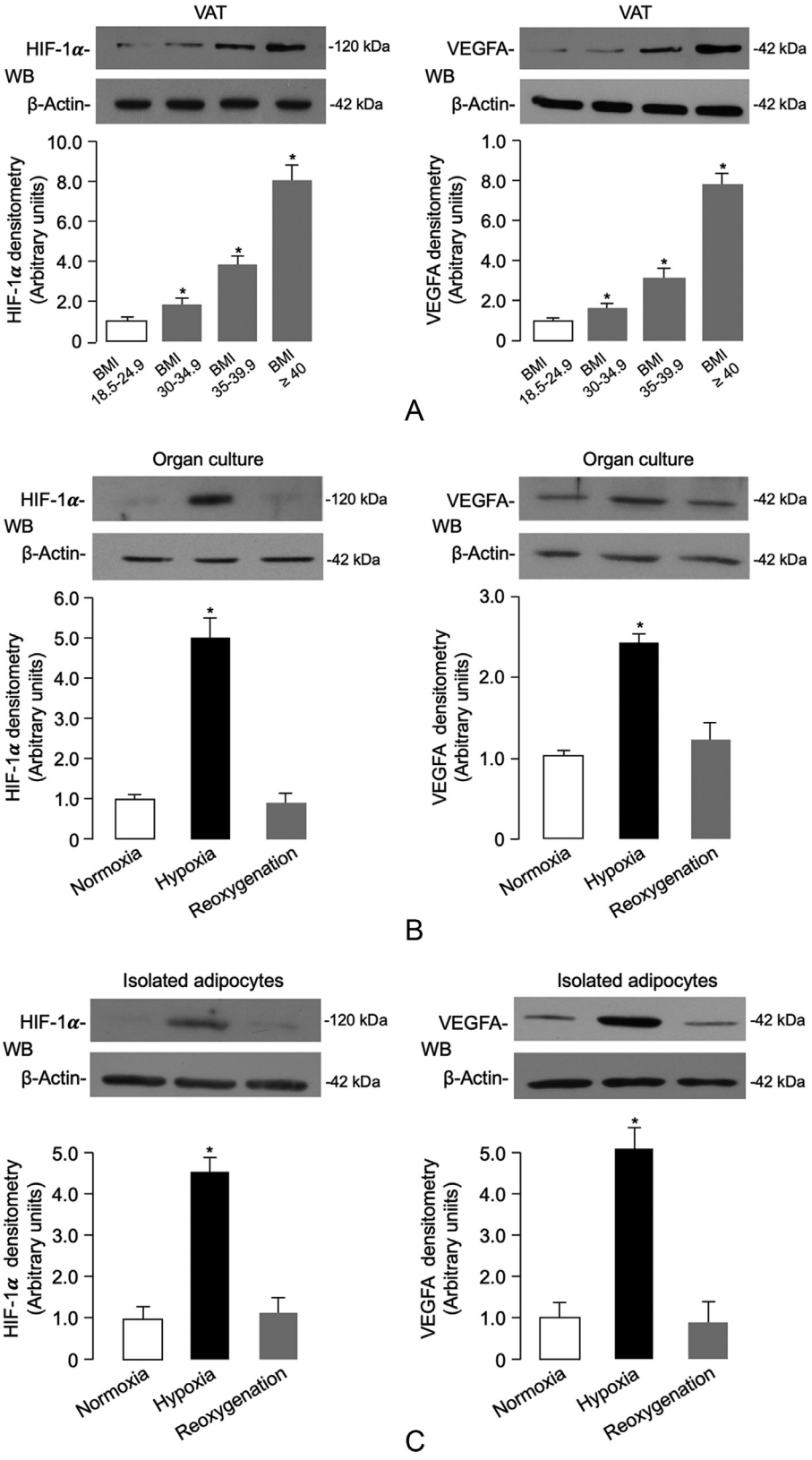

Fig. 2. Hypoxia-induced HIF-1α/VEGFA expression, INSR levels and signaling in VAT and isolated visceral adipocytes. (**A**) HIF-1α and VEGFA protein expression was measured by WB in whole VAT fragments from all subjects in each BMI group. BMI of 18.5−24.9 is representative of 20 normal-weight subjects; BMI 30−34.9 is representative of 7 obese subjects; BMI 35−39.9 is representative of 8 obese subjects; and BMI ≥ 40 is representative of 11 obese subjects. BMI bars are the mean ± *s*.e.m of densitometric analysis of WB results from each group. β-actin was the loading control. $^*P < 0.05$ *vs* normal-weight subjects [Student's *t*-test]. (**B,C**) HIF-1α and VEGFA protein expression was measured by WB in organ cultures and isolated adipocytes obtained from VAT of 12 normal-weight subjects, which were divided into groups of four each, and placed either in normoxia (7% O_2) or hypoxia (1% O_2) for 48 h. Reoxygenation was reestablished by placing hypoxic tissue/cells in normoxic conditions for 24 h. Representative WBs and mean densitometric analyses of WBs performed in organ cultures/isolated adipocytes under different oxygen tension (n = 4 independent samples per group) are shown. $^*P < 0.05$ *vs* normoxia [Student's *t*-test].

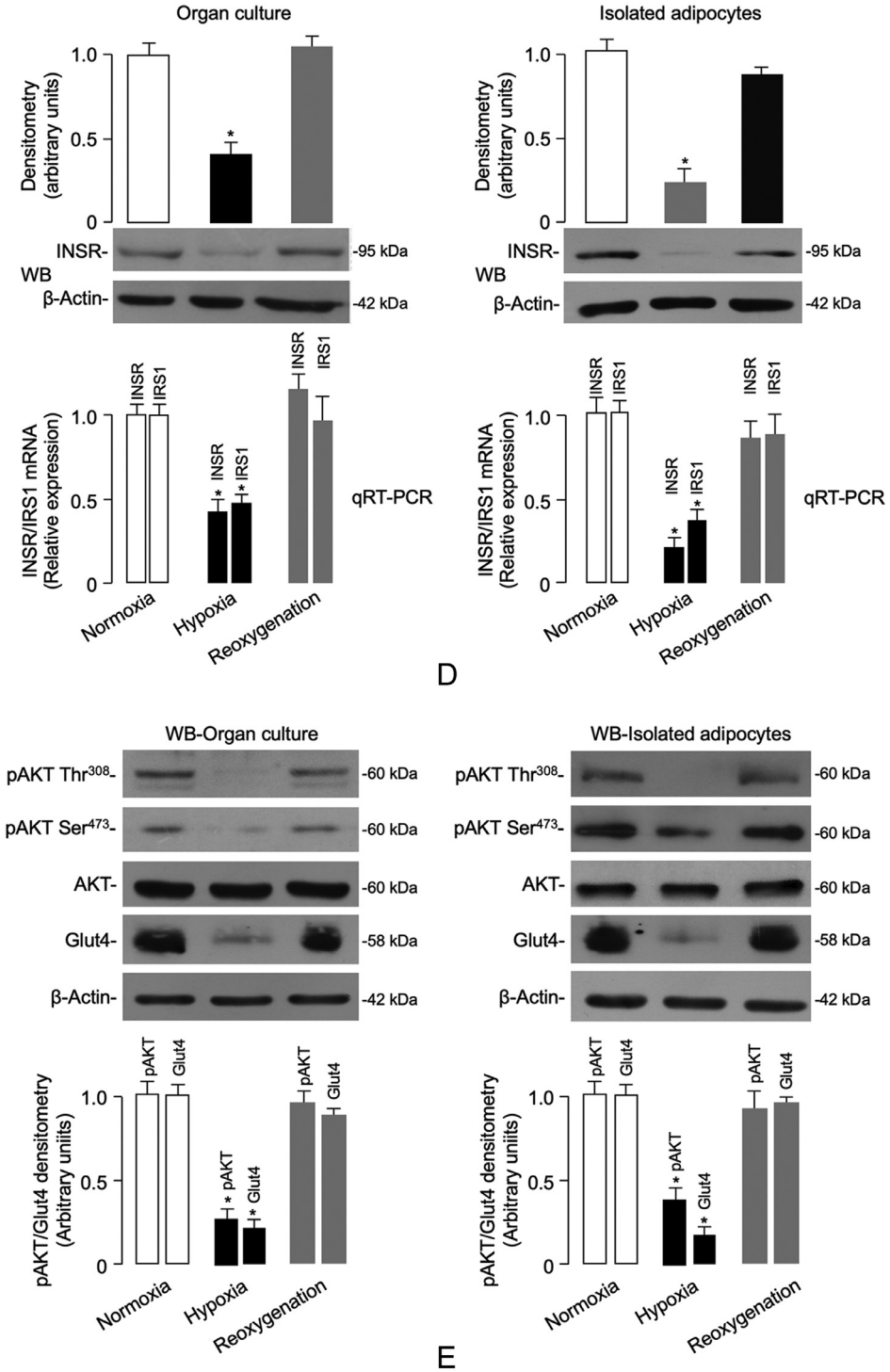

Fig. 2. (Continued)
(**D,E**) The expression levels of INSR, IRS1, total Akt and insulin-stimulated pAkt (Ser^{473}/Thr^{308}), and plasma membrane Glut4 content, were measured by RT-qPCR and/or WB in both organ culture tissue and isolated adipocytes from VAT samples of normal-weight subjects ($n = 4$ independent samples per group), under the same normoxic/hypoxic conditions as in (B,C). Representative WBs and mean densitometric analyses of WBs are shown. $^{*}P < 0.05$ vs normoxia [Student's *t*-test].

observed in hypoxia-exposed (1% O_2) 3T3-L1 adipocytes, when compared to cells under normoxic (7% O_2) conditions. This reduction paralleled the decrease in INSR protein levels, as detected by WB from cell lysates (Fig. 4b). The adverse effect produced by hypoxia on INSR expression was accompanied by a markedly reduction of both insulin-induced Ser^{473} and Thr^{308} Akt phosphorylation (pAkt), with no changes in total Akt protein abundance (Fig. 4b). Also in this case, reoxygenation of 3T3-L1 adipocytes following hypoxic treatment restored the expression of INSR and enhanced the levels of pAkt (Fig. 4b). As a consequence of the inhibition of insulin signaling, insulin-stimulated translocation of Glut4 to the plasma membrane was markedly reduced, and insulin failed to increase 2-deoxy-D-glucose (2-DG) uptake in 3T3-L1 adipocytes under hypoxic conditions (Fig. 4c), thereby further supporting the dependence of insulin signaling on the oxygen concentration in the cellular environment. As in the case of HFD-fed mice, this finding was corroborated by

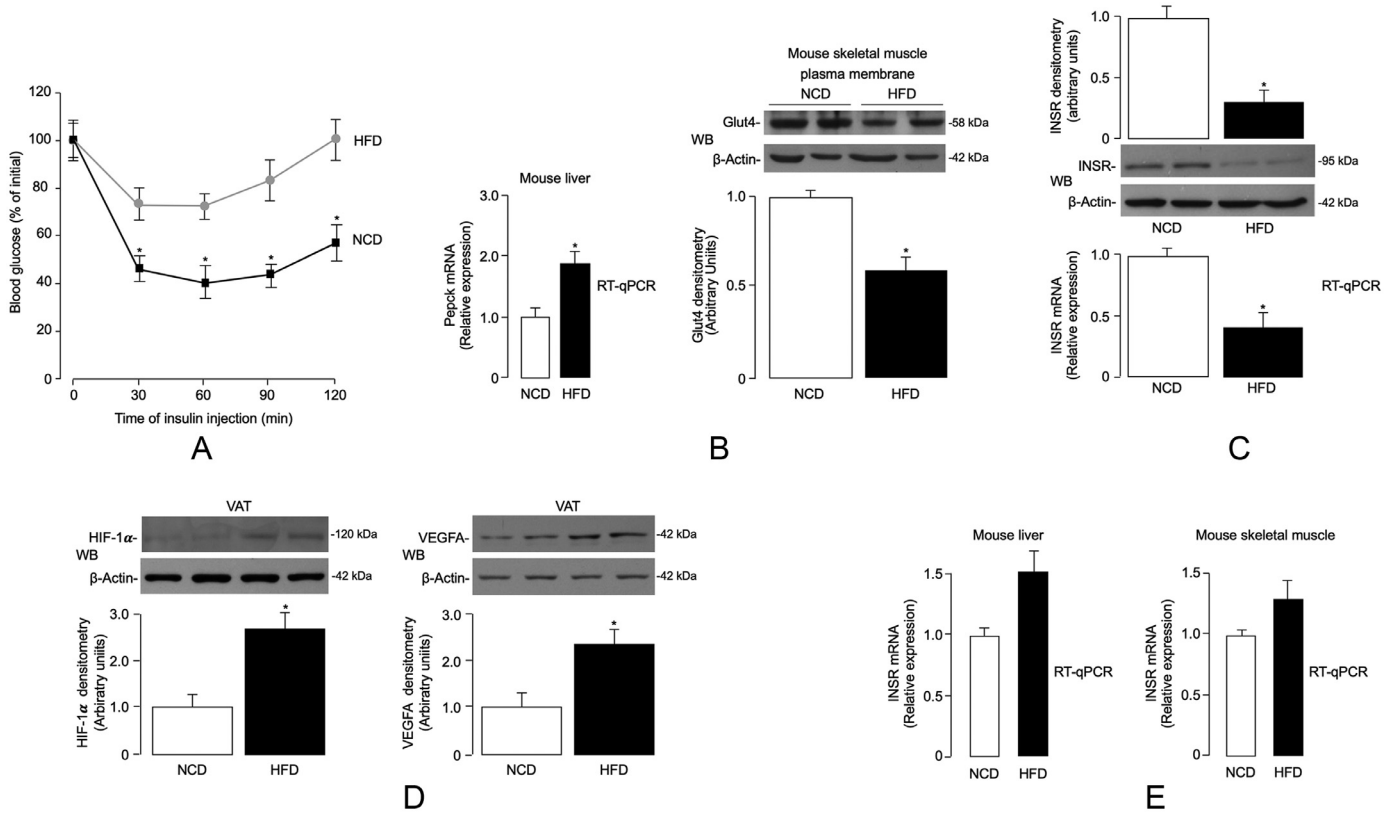

Fig. 3. ITT, Pepck, Glut4, HIF-1α/VEGFA and INSR expression in DIO mice. (**A**) ITT. Black squares, NCD mice (n = 10); gray circles, HFD mice (n = 10). Values are expressed as mean ± s.e.m. *$P < 0.05$ vs NCD mice [Student's t-test]. (**B**) Liver phosphoenolpyruvate carboxykinase (Pepck) mRNA, and Glut4 protein expression in skeletal muscle plasma membranes, as measured by RT-qPCR and WB analysis, respectively, in NCD (n = 10) and HFD (n = 10) mice. A representative WB is shown, together with densitometric analyses of multiple immunoblots (n = 10 animals for each group). *$P < 0.05$ vs NCD mice [Student's t-test]. (**C**) INSR mRNA and protein levels in VAT from NCD and HFD mice, as measured by RT-qPCR and WB, respectively. Data from each analysis are representative of 10 mice for each group. *$P < 0.05$ vs NCD mice [Student's t-test]. (**D**) HIF-1α and VEGFA protein expression in VAT from NCD (n = 10) and HFD (n = 10) mice, as measured by WB. β-actin, loading control. Representative WBs and mean densitometric analyses of WBs are shown. *$P < 0.05$ *vs* NCD [Student's t-test]. (**E**) INSR mRNA levels in liver and skeletal muscle from NCD (n = 10) and HFD (n = 10) mice, as measured in (C).

quantitative RT-qPCR analysis of Pepck mRNA in hypoxia-treated 3T3-L1 adipocytes, in which, as expected, no decrease in Pepck mRNA levels was observed following insulin treatment (Fig. 4c).

In an attempt to contribute to a fuller understanding of the mechanism(s) underlying hypoxia-induced inhibition of INSR expression, we next carried out reporter gene assays in which 3T3-L1 adipocytes were transfected transiently with the Luc reporter construct, pGL3-INSR-Luc, containing the INSR gene promoter upstream of the reporter gene. As shown in Fig. 4d, in normoxia vs hypoxia, no changes in Luc activity were observed in 3T3-L1 cells transfected with the pGL3-INSR-Luc reporter vector. These data indicate that hypoxia might negatively affect INSR expression in adipocytes through a post-transcriptional mechanism that involves cellular mRNA structure (for example, folding) and mRNA stability, rather than a mechanism of transcriptional inactivation of gene expression. To determine whether hypoxia was involved in post-transcriptional processes affecting INSR expression, we then examined the half-life of INSR mRNA in 3T3-L1 cells exposed to or not exposed to hypoxia. As shown in Fig. 4e, INSR mRNA half-life decreased from ~7 h in normoxic control cells to just over 2 h in cells under hypoxic conditions, suggesting that cellular hypoxia may indeed have a major influence in downregulating INSR expression. The potential post-transcriptional mechanism(s) by which hypoxia could induce downregulation of INSR mRNA were further investigated in 3T3-L1 adipocytes subjected to hypoxia and reoxygenation conditions, in which ongoing general transcription was inhibited by the addition of actinomycin D [62]. As shown in Fig. 4f, exposure of cells to hypoxia for 8 h decreased INSR mRNA levels to the same extent in the presence as in the absence of actinomycin D, indicating that the reduction in INSR expression was not via transcription. In contrast, the enhanced expression of INSR mRNA following reoxygenation appeared to be the result of upregulated transcription (Fig. 4f). Taken together, our findings point to a mechanism by which hypoxia-induced downregulation of INSR expression in adipocytes could be mediated by the enhancement of either miRNAs and/or mRNAs encoding for proteins that induce mRNA instability/degradation.

3.6. Hypoxia-related miRNA expression in adipocytes

A number of mechanisms have been proposed through which translational repression may occur in most cellular contexts in mammals. Central, among these mechanisms, is the fundamental role of miRNAs, an evolutionarily conserved class of short non-coding RNAs, that regulate gene expression post-transcriptionally [63,64]. Recently, consensus has been reached that mRNA destabilization and degradation is the dominant means of repression by miRNAs [65]. Based on these considerations and in an attempt to provide further insight into the mechanism(s) by which hypoxia adversely affects INSR mRNA stability and decay, we next undertook an in-depth study of miRNA expression profiles in hypoxic 3T3-L1 adipocytes compared with normoxic control cells. A set of miRNAs differentially expressed between normoxic and hypoxic conditions was identified (Fig. 5a). According to the computational-prediction analysis based on TargetScan (www.targetscan.org), we focused our attention on the miR-128 which was found to be one of the most upregulated miRNA in hypoxic 3T3-L1 adipocytes, directly targeting the 3′-UTR sequence of the *INSR* gene. In this regard, bioinformatic analysis for target gene

prediction was consistent with a previous report, in which a single putative miR-128 target site was identified in the 3′-UTR sequence of the *INSR* gene [66]. Time course analysis (not shown) in 3T3-L1 cells revealed that the induction of miR-128 occurred already at 1 h hypoxia, reached a 6–8-fold peak after 6–8 h, thereby preceding the decrease in INSR mRNA level that was not detected until 2 h of hypoxia, as shown in Fig. 4e.

In light of these data, we then hypothesized that the elevated levels of miR-128 under hypoxic conditions could play a role in hypoxia-mediated degradation and translation repression of INSR mRNA in the adipocytes of obese subjects. We first examined the levels of miR-128 in VAT from obese humans and mice. As shown in Fig. 5b, the level of miR-128 in visceral fat from both obese patients and HFD-fed mice was markedly and significantly higher than that from normal weight subjects and NCD-fed mice. The increase in miR-128 abundance coincided with the decrease in INSR expression in the same adipose tissues of humans and mice, indicating, therefore, that an inverse relationship between miR-128 and INSR indeed exists in both human and mouse obesity. No variations in miR-128 expression levels were instead observed in liver and skeletal muscle of HFD/obese mice when compared to NCD-fed control animals (Fig. 5c), indicating that overexpression of miR-128 in obesity is specific for VAT.

In order to demonstrate that hypoxia in obesity can directly induce miR-128 upregulation in visceral adipocytes, VAT fragments from 12 non-obese subjects were placed in organ culture for 48 h, in either normoxic or hypoxic conditions, and miR-128 was analyzed by RT-qPCR, as defined above. Also in this case, as shown in Fig. 5d, miR-128 was significantly higher in normal human adipose tissue samples maintained in hypoxic organ culture when compared with normoxic and reoxygenated tissues, which was consistent with the miR-128 expression level observed in hypoxic 3T3-L1 adipocytes.

HIF-1α is recognized as a major transcriptional regulator of gene expression in response to hypoxia. We then investigated the potential involvement of this factor in the induction of miR-128 in 3T3-L1 adipocytes. As shown in Fig. 5e, no effect of HIF-1α [40] was observed in relation to endogenous miR-128 levels in these cells, thereby indi-

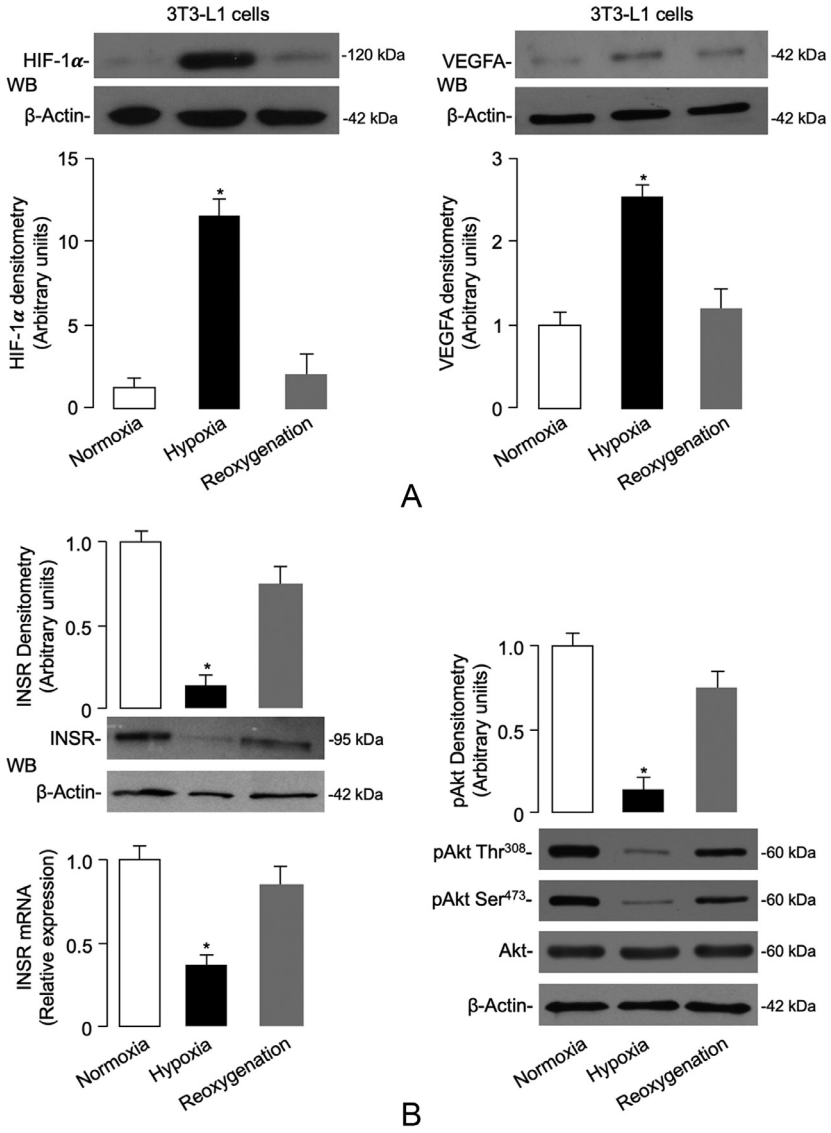

Fig. 4. Hypoxia-induced changes in INSR expression, and insulin signaling and INSR mRNA decay in mouse 3T3-L1 adipocytes. (**A**) HIF-1α and VEGFA mRNA and protein expression were measured in 3T3-L1 adipocytes that underwent hypoxia and hypoxia/reoxygenation for 48 h. Data for RT-qPCR and WB are representative of at least 3 independent experiments in duplicate for each condition tested. $^*P < 0.05$ vs control cells (normoxia) [Student's *t*-test]. (**B**) INSR mRNA levels and protein expression, and total Akt and pAkt (Ser^{473}/Thr^{308}) in normoxic and hypoxic 3T3-L1 adipocytes, as measured by RT-qPCR and WB, under the same experimental conditions as in (A). Mean densitometric analysis of four to six immunoblots for INSR and pAkt is shown. $^*P < 0.05$ *vs* normoxia [Student's *t*-test].

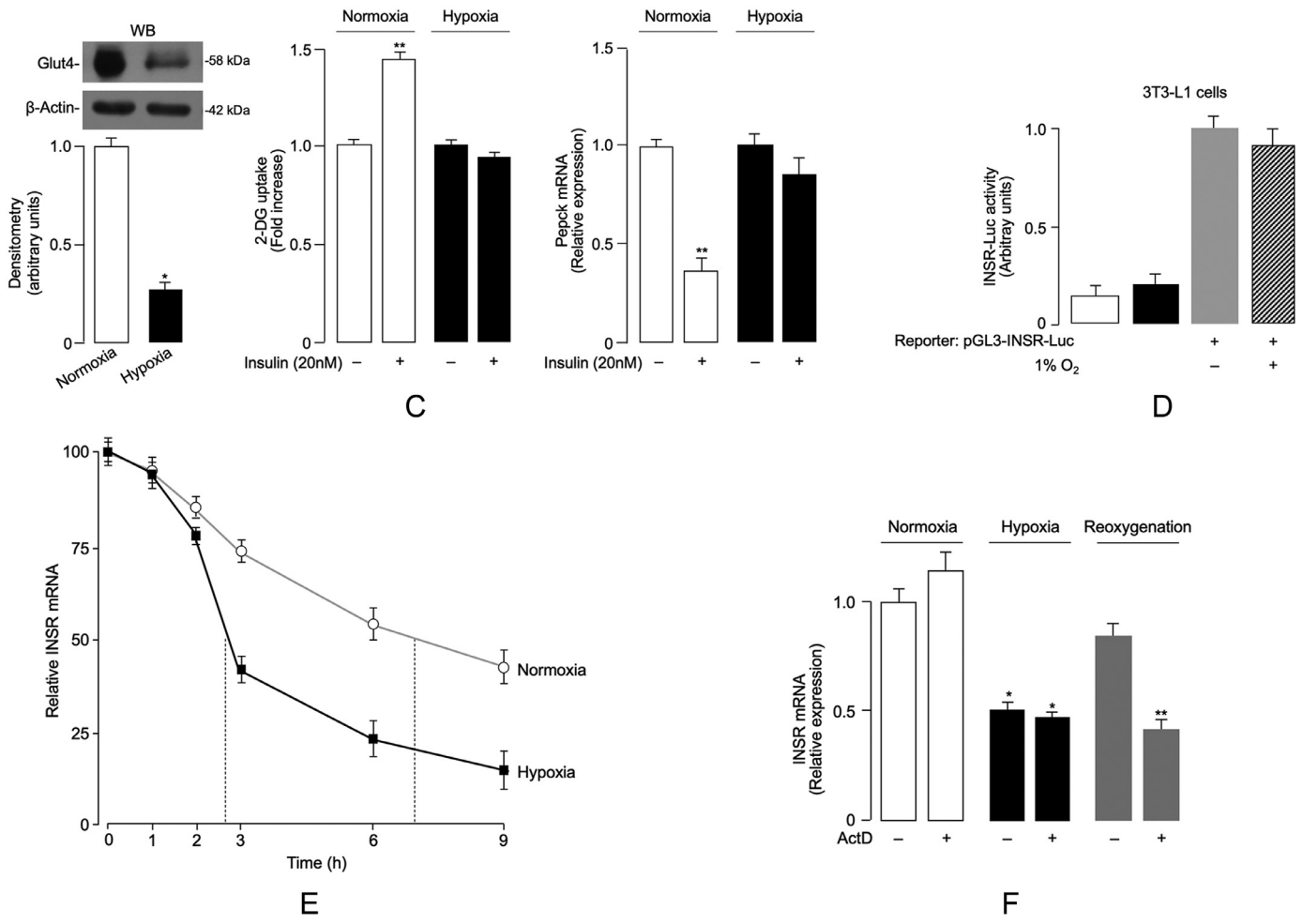

Fig. 4. (Continued)
(**C**) Glut4 protein content and the effect of insulin on 2-deoxy-D-glucose (2DG) uptake and Pepck mRNA levels in differentiated 3T3-L1 adipocytes under normoxic and hypoxic conditions. A representative WB of Glut4 in plasma membrane is shown, together with densitometric analysis. Data are means ± *s*.e.m. of 3 independent experiments, each in replicates of 3. $^{*}P < 0.05$ vs normoxia; $^{**}P < 0.05$ vs normoxic insulin-free cells [Student's *t*-test]. (**D**) pGL3-INSR Luciferase (Luc) reporter plasmid (300 ng) was transfected into differentiated 3T3-L1 adipocytes, incubated either in normoxia or hypoxia for 48 h, and Luc-activity was measured 48 h later. Data are means ± s.e.m. for 3 separate experiments performed in duplicate. Values in hypoxia (dashed bar) are expressed relative to the Luc activity obtained in transfections with the pGL3-INSR Luc in normoxic condition (gray bar), which is assigned an arbitrary value of 1. White bar, mock (no DNA); black bar, pGL3-vector without an insert. (**E**) INSR mRNA decay in differentiated 3T3-L1 cells, cultured in normoxic (open circles) and hypoxic (solid squares) conditions. Results are the mean ± s.e.m. of triplicates from 3 separate assays. (**F**) Hypoxia/reoxygenation-mediated effects on INSR mRNA. After 24 h exposure to hypoxia alone, 3T3-L1 mature adipocytes were treated or not with actinomycin D (ActD, 2 μg/mL) and cells were subjected to hypoxia or reoxygenation for further 8 h. Cells in normoxia, with or without ActD, cultured for the same time period, served as control. RT-qPCR was performed to quantify INSR mRNA levels. Results are the mean ± s.e.m. of triplicates from 3 separate experiments. $^{*}P < 0.05$ vs normoxia; $^{**}P < 0.05$ vs cells under reoxygenation, without (−) ActD [Student's *t*-test].

cating that hypoxia-induced miR-128 was independent from this transcription factor.

3.7. *Effect of miR-128 on INSR expression*

In order to further investigate the biological role of miR-128 and increase our understanding of the inverse relationship observed between miR-128 and INSR expression in VAT of both humans and mice, we next carried out transient transfections of miR-128 in 3T3-L1 adipocytes, in which endogenous expression of INSR is naturally induced upon adipocyte cell differentiation [67,68]. As shown in Fig. 6a, overexpression of a miR-128 mimic markedly inhibited the expression levels of both INSR mRNA and protein in normoxic transfected 3T3-L1 cells, but did not interfere with this process in HEK-293 cells, where INSR expression was unaffected (Fig. 6a). These observations suggest that the effects of miR-128 at the 3′-UTR of INSR are cell-type specific and might be influenced by either *cis* and/or *trans* factors which are differentially expressed in specific cell types. In support of the specificity of this result, no differences were found in INSR mRNA and protein levels in cell transfections with a miR-128 inhibitor (Fig. 6a). The lack of effect of miR-128 mimic on INSR expression in HEK-293 cells was apparently not in line with a previous study in which transient miR-128 overexpression in this cell model was able to inhibit the reporter activity of an INSR gene-Luc construct [66]. The two studies, however, differ for both technical background and scope. In our study, we tried to address a physiological issue by testing the effect of miR-128 on the expression of endogenous INSR in two cell types, 3T3-L1 adipocytes and HEK-293 cells, which are typical and less typical insulin targets, respectively. To further support the adipose cell-specific effect of miR-128 on the reduction of INSR mRNA and protein production, we finally carried out experiments with 3T3-L1 adipocytes, which were preincubated under hypoxic conditions in the presence of mir-128 mimic or miR-128 inhibitor. As shown in Fig. 6b, it was confirmed that hypoxia alone greatly weakened INSR mRNA and protein expression levels, and this effect was even more pronounced when the combined hypoxia/miR-128 treatment was carried out simultaneously. Interestingly, and most relevant to this issue, the abundance of INSR, both in terms of mRNA and protein, was almost

miRNAs	
Overexpressed	**Underexpressed**
hsa-miR-433	hsa-miR-514
hsa-miR-520h	hsa-miR-520e
hsa-miR-153	hsa-miR-1275
hsa-miR-128	hsa-miR-141
hsa-miR-579	hsa-miR-17-5p
	hsa-miR-132
	hsa-miR-141
	hsa-miR-221
	hsa-miR-184
	hsa-miR-196
	hsa-miR-518
	hsa-miR-337

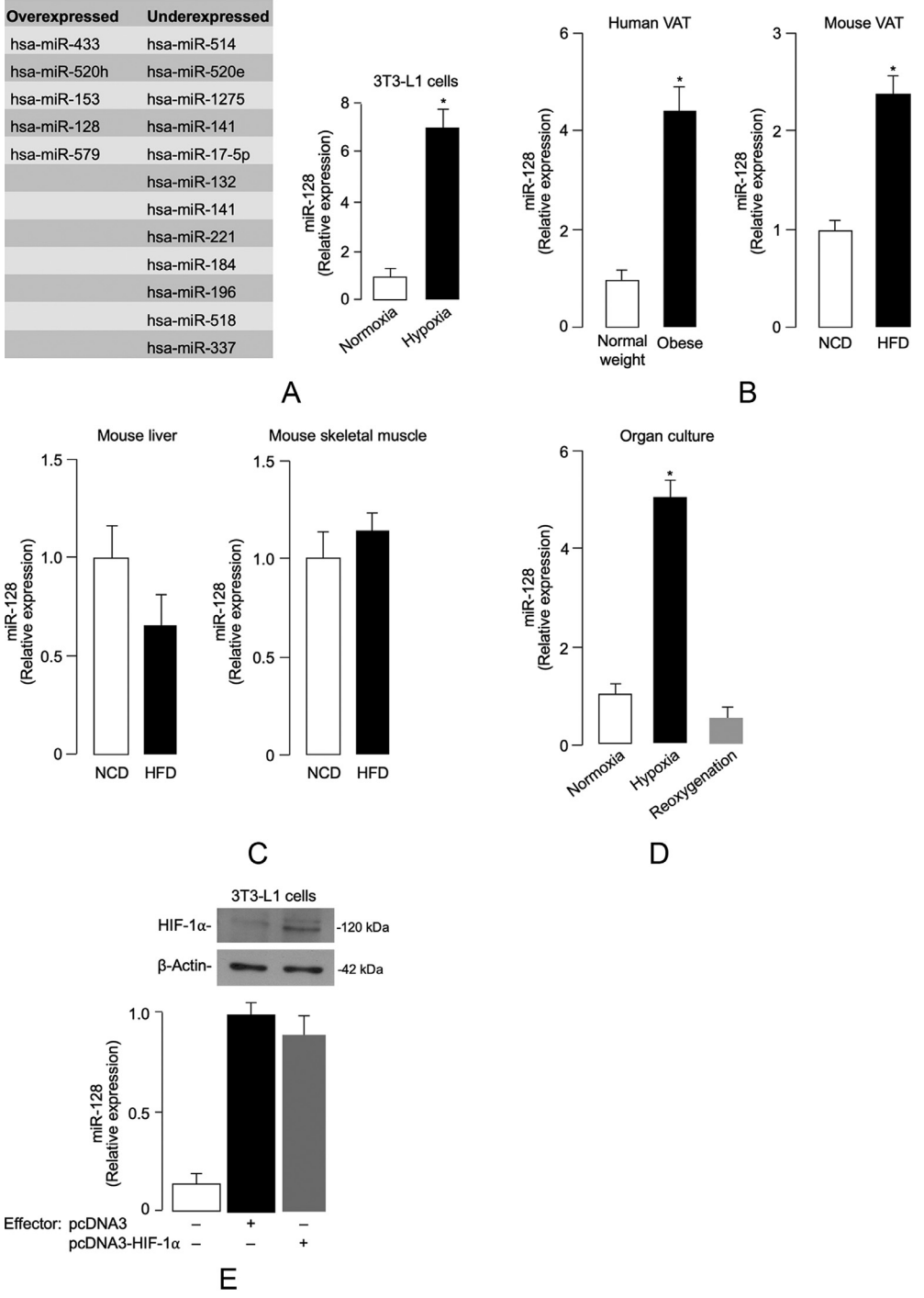

Fig. 5. Hypoxia-related miRNA expression. (**A**) Differentially expressed miRNAs in hypoxic 3T3-L1 adipocytes vs normoxic cells. miRNAs whose expression was either upregulated (> 2-fold) or downregulated (< 0.5) after hypoxia treatment (1% O_2) of cells are shown in the diagram (left). The expression levels of miR-128 in normoxic and hypoxic 3T3-L1 adipocytes were determined by RT-qPCR (right); results are the means ± s.e.m. from 3 independent experiments, each in triplicate; $P < 0.001$ vs normoxia [Student's *t*-test]. (**B**) miR-128 expression in VAT from normal-weight and obese individuals ($n = 10$ per each group), and mice under NCD- and HFD-fed conditions ($n = 10$ per each group) for 15 weeks. In the obese subject category, VAT samples were as follows: 3 (BMI 30−34.9); 3 (BMI 35−39.9); 4 (BMI ≥ 40). Data are the means ± s.e.m. of 2 independent RT-qPCR assays from each individual tissue sample. $^*P < 0.05$ vs control (white bar) [Student's *t*-test]. (**C**) miR-128 levels in liver and skeletal muscle from NCD- and HFD-fed mice as measured in (B). (**D**) miR-128 levels as measured by RT-qPCR in VAT from normal-weight, non-obese individuals ($n = 10$), placed in organ culture for 48 h, either in normoxic or hypoxic environment, or after reoxygenation. $P < 0.001$ *vs* normoxia [Student's *t*-test]. (**E**) Normoxic 3T3-L1 adipocytes were transiently transfected with an effector plasmid (1 μg) expressing HIF-1α. After 48 h, miR-128 levels were measured by RT-qPCR. Results are the mean ± s.e.m. of triplicates from 3 independent assays. A representative WB of HIF-1α is shown for each condition. White bar, mock (no DNA); black bar, pcDNA3-vector without an insert; gray bar, pcDNA3-HIF-1α effector vector.

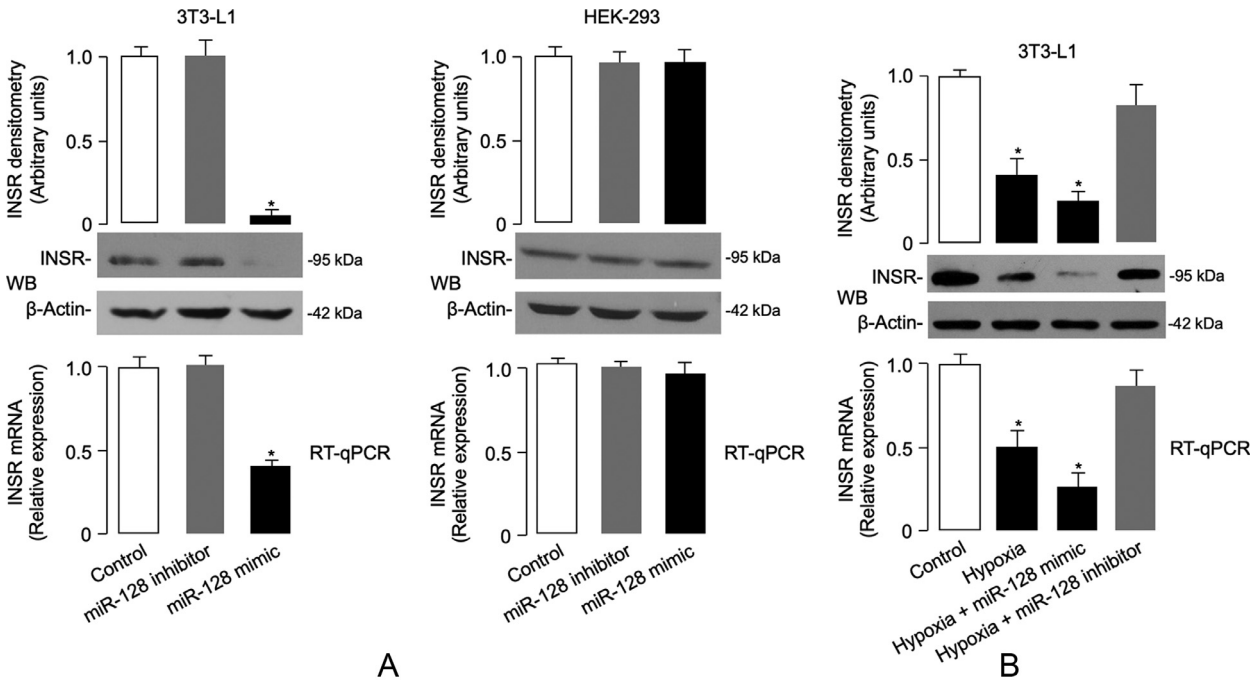

Fig. 6. miR-128 and INSR expression. (**A**) Determination of endogenous INSR mRNA and protein expression levels in 3T3-L1 adipocytes and HEK-293 cells transfected with either a miR-128 inhibitor or mimic by RT-qPCR and WB, respectively. (**B**) Endogenous INSR mRNA and protein expression levels were measured as in (A), in 3T3-L1 adipocytes transfected with miR-128 mimic or miR-128 inhibitor and exposed to hypoxia for 48 h before INSR expression was determined. Representative WBs are shown. β-actin, control of protein loading. Densitometric scanning of INSR protein signals are shown in bar graphs. Results in (A,B) are representative of at least 3 independent experiments, each in triplicate: bars are mean ± s.e.m. $^*P < 0.05$ vs normoxic untransfected cells (control, white bar) [Student's *t*-test].

unchanged and remained similar to its level in normoxic conditions when hypoxic 3T3-L1 adipocytes were preincubated with miR-128 inhibitor (Fig. 6b).

3.8. Adipose-derived serum biomarkers of insulin resistance

All of the above data further support the role of adipose tissue dysfunction in the pathogenesis of systemic insulin resistance. We next determined whether the observed reductions in INSR expression and insulin signaling in human VAT were associated with alterations in the production of adipose-derived serum factors which may contribute to systemic insulin resistance by impairing insulin signaling in liver and skeletal muscle. In the four study groups of patients with different ranges of BMI we measured the circulating levels of adipokines, cytokines and other analytes which are typically dysregulated in obesity-related insulin resistance. As shown in Table 2, among the adipokines, the insulin-sensitizing adiponectin was significantly reduced. In contrast, resistin and RBP-4, which interfere with insulin-induced glucose uptake by skeletal muscle and amplify hepatic glucose release [58,69], increased during the progression from mild to severe and very severe obesity. Also, pro-inflammatory factors, including CRP, and cytokines, such as IL-6, TNF-α, and INF-γ, which contribute to insulin resistance in obese individuals [9,11], increased with adipometrics. In addition, VEGF, as well as MCP-1, an inflammatory chemokine with insulin-resistance-inducing capacity [9,70], increased with obesity in a continuous fashion. Although not statistically significant, an analogous trend was observed for IL-8, another inflammatory marker linked to insulin resistance in obesity [9,70]. Thus, these results are compatible with the concept that, during the progression to more severe degrees of obesity, the impairment of INSR expression and INSR signal transduction, in VAT, parallels adipose-tissue dysfunction, secondarily leading to insulin resistance in liver and skeletal muscle. Remarkably, these data

Table 2
Serum levels of adipokines, cytokines and other related laboratory parameters in the study groups.

	Controls BMI 18.5–24.9A	Group 1 BMI 30–34.9 B	Group 2 BMI 35–39.9 C	Group 3 BMI ≥ 40D	*p*
Number, *n*	20	7	8	11	–
Adiponectin, μg/mL	8.0 ± 3.5	5.5 ± 3.1	4.4 ± 1.6	2.8 ± 1.5	< 0.001
Leptin, pg/mL	15.6 ± 7.8	31.1 ± 19.2	52.4 ± 11.0	66.4 ± 12.6	< 0.001
Resistin, pg/mL	3.5 ± 2.2	5.2 ± 0.9	5.3 ± 1.7	6.1 ± 2.3	0.011
RBP-4, g/mL	38.0 ± 0.6	43.7 ± 0.6	49.7 ± 0.7	58.2 ± 0.9	< 0.001
hs-CRP, mg/L	1.1 ± 0.6	2.5 ± 2.1	5.3 ± 4.7	9.0 ± 7.1	< 0.001
IL-6, pg/mL	0.9 ± 0.8	1.6 ± 0.6	2.2 ± 1.0	2.9 ± 1.1	< 0.001
TNF-α, pg/mL	2.9 ± 1.9	4.1 ± 2.0	6.4 ± 4.5	7.9 ± 4.2	0.003
INF-γ, pg/mL	1.8 ± 1.1	2.9 ± 2.5	4.0 ± 3.9	4.8 ± 3.3	0.021
MCP-1, pg/mL	157.6 ± 46.6	179.1 ± 54.3	236.1 ± 64.8	268.0 ± 58.9	< 0.001
IL-8, pg/mL	11.7 ± 7.6	16.4 ± 11.3	20.0 ± 19.0	24.6 ± 15.6	0.078
VEGF, pg/mL	162.6 ± 70.0	269.7 ± 117.9	302.2 ± 108.7	330.1 ± 86.7	< 0.001

Data are mean ± SD or number (*n*). Kruskall–Wallis test was employed for continuous values comparisons.

indicate that serum levels of a number of adipokines and markers of inflammation also correlate with the different stages of obesity development. The link between various adipokines and insulin resistance and type 2 diabetes has been widely reported [14]. However, it remains to be determined whether the changes in these adipocytokines across the different stages of obesity may contribute to the progressive decline of INSR expression and signaling in VAT of obese individuals. Further studies in this field will help clarify the relevance of these molecules on BMI-dependent inhibition of INSR.

4. Discussion

The integrity of the INSR signaling in adipose tissue is crucial for the maintenance of whole-body glucose and lipid homeostasis, as well as peripheral insulin sensitivity. This notion is well supported by studies in experimental animal models with adipose-specific ablation of INSR (or its downstream IRS signaling molecules), in which peripheral insulin resistance occurs in skeletal muscle and liver due to adipocyte and adipose tissue dysfunction [26,27,71,72]. On the other hand, it has been found that selective downregulation of GLUT4 in adipose tissue of obese animals and humans correlates inversely with peripheral insulin sensitivity, representing a prominent feature of insulin-resistant states, including T2D [37,58–60,73]. However, despite the current evidence, the molecular mechanisms underlying the adverse effects of obesity on INSR signaling have not yet been fully explained. In the present study therefore, in order to more closely understand this issue, we performed studies of INSR expression and insulin signaling both in vivo, in obese humans and mice, and in vitro, in human and murine adipocyte cultures.

For the first time, we now provide experimental evidence on the inverse relationship between increasing BMI and decreasing INSR expression and insulin signaling in human VAT during the progression from normal weight to mild and severe obesity. Our data extend previous observations showing that hypoxia, a well-established characteristic feature of obese adipose tissue [74], plays a determinant role in this scenario, as demonstrated by the results from immunoblots and RT-qPCR of VAT fragments and isolated visceral adipocytes from normal-weight subjects, in which hypoxia-induced downregulation of INSR expression was reversed by restoration of oxygen supply. The decrease in INSR expression in VAT of obese subjects was replicated in subsequent experiments with HFD-induced model of obesity in mice, in which INSR in VAT was considerably reduced with respect to that found in normal weight mice. Interestingly, this reduction appeared to be tissue-specific, given that mouse obesity had no effect on INSR mRNA in liver and skeletal muscle, supporting the hypothesis that impaired INSR signaling in liver and muscle of this mouse model of obesity, is presumably due to post-receptor site alterations, being developed as a consequence of the adipose tissue dysfunction.

The direct effect of hypoxia on INSR levels was supported by our findings in cultured 3T3-L1 adipocytes, in which low oxygen tension adversely affected INSR protein expression by inducing miR-128 upregulation and subsequently accelerating INSR mRNA decay. Since the increase of miR-128 levels in VAT correlated with the decrease in INSR expression in the same tissues, it is plausible to presume that hypoxia-induced downregulation of INSR in obese human and mouse adipocytes is mediated, at least in part, by miR-128. This mechanistic explanation is corroborated by our results obtained using normoxic and hypoxic 3T3-L1 adipocytes transfected with miR-128 mimic or anti-miR-128, and is supported by data from computational prediction analysis suggesting the INSR as a potential target of miR-128. In addition, such a mechanistic view is in line with previous studies in the context of breast cancer tumorigenesis, showing that the expression levels of INSR and its downstream IRS1 target were reduced in breast cancer cell lines overexpressing miR-128 [75].

Overall, our findings well support the notion that hypoxia in obese adipose tissue may play a critical role in the impairment of peripheral insulin action and development of systemic insulin resistance. In line with this notion is our observation that several proinflammatory cytokines and adipokines that are known to influence insulin signaling in liver and skeletal muscle were significantly altered in serum of obese subjects, compared to serum of normal-weight individuals. In a previous study in vitro [55], it was reported that hypoxia was able to decrease INSR signaling in cultured adipocytes. However, unlike in our study, that study did not find a reduction in cellular INSR protein expression. It is possible that the discrepancy between the two studies, at this level, may be explained on the basis of the different experimental conditions employed. For example, a particularly pertinent issue in this context, is the O_2 level that is required to create the condition of normoxia or hypoxia in vitro. In our study, both 3T3-L1 and isolated human visceral adipocytes were incubated in 7% O_2, which is considered within the physiological normoxic range in studies with human adipocytes in culture [9], thus considerably lower than the 21% O_2 under which adipocytes were incubated in the other study. Furthermore, in our in vitro experiments, cells were exposed to hypoxia for a longer period of time (48 h), in comparison with the other study (16 h) [55]. Therefore, it is reasonable to suppose that in our cellular models, longer exposure to hypoxia may result in INSR downregulation in a manner analogous to the progressive downregulation of INSR expression observed in vivo, in VAT of obese subjects, during the progression from normal weight to mild and severe obese status. Indeed, in line with our results, a significant decrease in INSR expression was reported in a previous study in hypoxic 3T3-L1 adipocytes [52]. In this latter case, the relevance of a longer exposure of cells to hypoxia was also underscored in time-course experiments, in which the reduction in cellular INSR protein expression was only detectable after 24 h of hypoxia treatment [52].

In summary, in the present study for the first time, we provide compelling evidence showing that an inverse correlation exists between the degree of BMI, INSR expression and insulin signaling in human VAT during the progression from normal weight to mild and severe obesity. We consider a novelty in the literature the progressive reduction of INSR expression in human VAT and the mechanism underlying this reduction, as we have not found previous studies that quantified the expression of INSR during obesity progression, and its negative relationship with hypoxia. Furthermore, the inverse correlation between the expression levels of INSR signaling components and plasma glucose/insulin levels across the different stages of obesity is another novelty of this study. This, together with the observation that a number of adipokines and markers of inflammation also correlate with these molecular and metabolic changes during individuals' transition from mild to very severe obesity, further contributes to the notion that visceral fat accumulation, via adipokine dysregulation and inflammation, represents a link between abdominal obesity and insulin resistance.

From a mechanistic point of view, our findings point to a pathogenic cascade of events, in which obesity-induced hypoxia increases the expression of miR-128, which in turn negatively affects INSR mRNA and protein expression levels in VAT, thus precluding insulin-stimulated glucose uptake by adipose tissue itself. Impaired glucose uptake in adipocytes may then contribute to secondary systemic insulin resistance through the abnormal release of adipose-derived adipokines, as well as proinflammatory mediators, which adversely affect insulin action in liver and skeletal muscle. Our observation that hypoxia-associated changes in the expression profiles of INSR and other insulin signaling components are restored by reoxygenation also in organ cultures of human VAT indicates that obesity-related VAT dysfunction is not permanent and can be reversed. In this respect, adipose-specific inhibition of miR-128 may constitute a strategy to ameliorate insulin resistance in obesity.

Declaration of Competing Interest

The authors declare no conflicts of interest.

Acknowledgments

We thank Dr. G.L. Semenza (Johns Hopkins University, Baltimore, USA) for providing the pcDNA3.1/HA-HIF-1α plasmid. Also, we thank Drs. N. De Grazia and S. Aidala, and Mrs A. Foti, M. Ciaccio and M. Fava for their support in biopsy examinations.

Funding sources

This work was partly supported by a grant from NUTRAMED 16 (PON 03PE000_78_1 to B.A.) and by the European Commission (FESR FSE 2014-2020 and Regione Calabria to M.M.). Funders did not have any role in study design, data collection, data analysis, interpretation, or writing of the report. The APC was funded by the Department of Health Sciences, University "Magna Græcia" of Catanzaro, Italy.

Supplementary materials

Supplementary material associated with this article can be found, in the online version, at doi:10.1016/j.ebiom.2020.102912.

References

[1] Flegal KM, Carroll MD, Kit BK, Ogden CL. Prevalence of obesity and trends in the distribution of body mass index among US adults, 1999-2010. J Am Med Assoc 2012;307:491–7.
[2] Kahn SE, Hull RL, Utzschneider KM. Mechanisms linking obesity to insulin resistance and type 2 diabetes. Nature 2006;444:840–6.
[3] Reaven GM. The insulin resistance syndrome: definition and dietary approaches to treatment. Annu Rev Nutr 2005;25:391–406.
[4] Kershaw EE, Flier JS. Adipose tissue as an endocrine organ. J Clin Endocrinol Metab 2004;89:2548–56.
[5] Greco M, Chiefari E, Montalcini T, Accattato F, Costanzo FS, Pujia A, et al. Early effects of a hypocaloric, mediterranean diet on laboratory parameters in obese individuals. Mediat Inflamm 2014;2014:750860.
[6] Arcidiacono B, Iiritano S, Nocera A, Possidente K, Nevolo MT, Ventura V, et al. Insulin resistance and cancer risk: an overview of the pathogenetic mechanisms. Exp Diabetes Res 2012;2012:789174.
[7] Lumeng CN, Saltiel AR. Inflammatory links between obesity and metabolic disease. J Clin Investig 2011;121:2111–7.
[8] Xu H, Barnes GT, Yang Q, Tan G, Yang D, Chou CJ, et al. Chronic inflammation in fat plays a crucial role in the development of obesity-related insulin resistance. J Clin Investig 2003;112:1821–30.
[9] Trayhurn P. Hypoxia and adipose tissue function and dysfunction in obesity. Physiol Rev 2013;93:1–21.
[10] Goossens GH. The role of adipose tissue dysfunction in the pathogenesis of obesity-related insulin resistance. Physiol Behav 2008;94:206–18.
[11] Hotamisligil GS. Inflammation and metabolic disorders. Nature 2006;444:860–7.
[12] Abel ED, Peroni O, Kim JK, Kim YB, Boss O, Hadro E, et al. Adipose-selective targeting of the GLUT4 gene impairs insulin action in muscle and liver. Nature 2001;409:729–33.
[13] Yudkin JS, Eringa E, Stehouwer CD. Vasocrine signalling from perivascular fat: a mechanism linking insulin resistance to vascular disease. Lancet 2005;365:1817–20.
[14] Saxton SN, Clark BJ, Withers SB, Eringa EC, Heagerty AM. Mechanistic links between obesity, diabetes, and blood pressure: role of perivascular adipose tissue. Physiol Rev 2019;99:1701–63.
[15] Sinha R, Dufour S, Petersen KF, LeBon V, Enoksson S, Ma YZ, et al. Assessment of skeletal muscle triglyceride content by ^{1}H nuclear magnetic resonance spectroscopy in lean and obese adolescents. Diabetes 2002;51:1022–7.
[16] Miljkovic I, Cauley JA, Petit MA, Ensrud KE, Strotmeyer E, Sheu Y, Gordon CL, et al. Greater adipose tissue infiltration in skeletal muscle among older men of african ancestry. J Clin Endocrinol Metab 2009;94:2735–42.
[17] Jones A, Danielson KM, Benton MC, Ziegler O, Shah R, Stubbs RS, et al. miRNA signatures of insulin resistance in obesity. Obesity 2017;25:1734–44.
[18] Ying W, Riopel M, Bandyopadhyay G, Dong Y, Birmingham A, Seo JB, et al. Adipose tissue macrophage-derived exosomal miRNAs can modulate in vivo and in vitro insulin sensitivity. Cell 2017;171:372–84.
[19] Castaño C, Kalko S, Novials A, Párrizas M. Obesity-associated exosomal miRNAs modulate glucose and lipid metabolism in mice. Proc Natl Acad Sci USA 2018;115:12158–63.
[20] Goldfine ID. The insulin receptor: molecular biology and transmembrane signalling. Endocr Rev 1987;8:235–55.
[21] White MF. Insulin signaling in health and disease. Science 2003;302:1710–1.
[22] Saltiel AR, Kahn CR. Insulin signalling and the regulation of glucose and lipid metabolism. Nature 2001;414:799–806.
[23] Freidenberg GR, Henry RR, Klein HH, Reichart DR, Olefsky JM. Decreased kinase activity of insulin receptors from adipocytes of non-insulin-dependent diabetic subjects. J Clin Investig 1987;79:240–50.
[24] Trischitta V, Wong KY, Brunetti A, Scalisi R, Vigneri R, Goldfine ID. Defects in insulin-receptor internalization and processing in monocytes of obese subjects and obese NIDDM patients. Diabetes 1989;38:1579–84.
[25] Ramalingam L, Oh E, Thurmond DC. Novel roles for insulin receptor (IR) in adipocytes and skeletal muscle cells via new and unexpected substrates. Cell Mol Life Sci 2013;70:2815–34.
[26] Boucher J, Softic S, El Ouaamari A, Krumpoch MT, Kleinridders A, Kulkarni RN, et al. Differential roles of insulin and IGF-1 receptors in adipose tissue development and function. Diabetes 2016;65:2201–13.
[27] Softic S, Boucher J, Solheim MH, Fujisaka S, Haering MF, Homan EP, et al. Lipodystrophy due to adipose tissue specific insulin receptor knockout results in progressive NAFLD. Diabetes 2016;65:2187–200.
[28] Srivastava A, Shankar K, Beg M, Rajan S, Gupta A, Varshney S, et al. Chronic hyperinsulinemia induced miR-27b is linked to adipocyte insulin resistance by targeting insulin receptor. J Mol Med 2018;96:315–31.
[29] W.H.O. Obesity: preventing and managing the global epidemic. Report of a WHO Consultation. World Health Organization Technical Report Series 2000; 894:1−253.
[30] Matthews DR, Hosker JP, Rudenski AS, Naylor BA, Treacher DF, Turner RC. Homeostasis model assessment: insulin resistance and beta-cell function from fasting plasma glucose and insulin concentrations in man. Diabetologia 1985;28:412–9.
[31] Caroleo M, Carbone EA, Primerano A, Foti D, Brunetti A, Segura-Garcia C. Brain-behavior-immune interaction: serum cytokines and growth factors in patients with eating disorders at extremes of the body mass index (BMI) spectrum. Nutrients 2019;11:1995.
[32] Carswell KA, Lee MJ, Fried SK. Culture of isolated human adipocytes and isolated adipose tissue. Methods Mol Biol 2012;806:203–14.
[33] Capobianco V, Nardelli C, Ferrigno M, Iaffaldano L, Pilone V, Forestieri P, et al. miRNA and protein expression profiles of visceral adipose tissue reveal miR-141/YWHAG and miR-520e/RAB11A as two potential miRNA/protein target pairs associated with severe obesity. J Proteome Res 2012;11:3358–69.
[34] Iacomino G, Siani A. Role of miRNAs in obesity and obesity-related diseases. Genes Nutr 2017;25(12):23.
[35] Arner P, Kulyte A. MicroRNA regulatory networks in human adipose tissue and obesity. Nat Rev Endocrinol 2015;11:276–88.
[36] Paonessa F, Foti D, Costa V, Chiefari E, Brunetti G, Leone F, et al. Activator protein-2 overexpression accounts for increased insulin receptor expression in human breast cancer. Cancer Res 2006;66:5085–93.
[37] Chiefari E, Paonessa F, Iiritano S, Le Pera I, Palmieri D, Brunetti G, et al. The cAMP-HMGA1-RBP4 system: a novel biochemical pathway for modulating glucose homeostasis. BMC Biol 2009;7:24.
[38] Wang CY, Liao JK. A mouse model of diet-induced obesity and insulin resistance. Methods Mol Biol 2012;821:421–33.
[39] Foti D, Chiefari E, Fedele M, Iuliano R, Brunetti L, Paonessa F, et al. Lack of the architectural factor HMGA1 causes insulin resistance and diabetes in humans and mice. Nat Med 2005;11:765–73.
[40] Messineo S, Laria AE, Arcidiacono B, Chiefari E, Luque Huertas RM, Foti DP, et al. Cooperation between HMGA1 and HIF-1 contributes to hypoxia-induced VEGF and visfatin gene expression in 3T3-L1 adipocytes. Front Endocrinol 2016;7:73.
[41] Laria AE, Messineo S, Arcidiacono B, Varano M, Chiefari E, Semple RK, et al. Secretome analysis of hypoxia-induced 3T3-L1 adipocytes uncovers novel proteins potentially involved in obesity. Proteomics 2018;18:1700260.
[42] Lo KA, Labadorf A, Kennedy NJ, Han MS, Yap YS, Matthews B, et al. Analysis of in vitro insulin-resistance models and their physiological relevance to in vivo diet-induced adipose insulin resistance. Cell Rep 2013;5:259–70.
[43] Corigliano DM, Syed R, Messineo S, Lupia A, Patel R, Reddy CVR, et al. Indole and 2,4-thiazolidinedione conjugates as potential anticancer modulators. PeerJ 2018;6:e5386.
[44] Brunetti A, Maddux BA, Wong KY, Hofmann C, Whittaker J, Sung C, et al. Monoclonal antibodies to the human insulin receptor mimic a spectrum of biological effects in transfected 3T3/HIR fibroblasts without activating receptor kinase. Biochem Biophys Res Commun 1989;165:212–8.
[45] Whelton PK, Carey RM, Aronow WS, Casey DE, Collins KJ, Dennison Himmelfarb C, et al. 2017 ACC/AHA/AAPA/ABC/ACPM/AGS/APhA/ ASH/ASPC/NMA/PCNA guideline for the prevention, detection, evaluation, and management of high blood pressure in adults: executive summary: a report of the American College of Cardiology/American Heart Association task force on clinical practice guidelines. Circulation 2018;138:e426–83.
[46] Chobanian AV, Bakris GL, Black HR, Cushman WC, Green LA, Izzo JL, et al. The seventh report of the joint national committee on prevention, detection, evaluation, and treatment of high blood pressure: the JNC 7 report. J Am Med Assoc 2003;289:2560–71.
[47] American Diabetes Association. 2. Classification and diagnosis of diabetes: standards of medical care in diabetes−2020, 2020. Diabetes Care 2020;43(Suppl. 1):S14–31.
[48] Third Report of the National Cholesterol Education Program (NCEP). Expert panel on detection, evaluation, and treatment of high blood cholesterol in adults (adult treatment panel iii) final report, 2002. Circulation 2002;;106:3143–421.
[49] Kang SG, Brown AL, Chung JH. Oxygen tension regulates the stability of insulin receptor substrate-1 (IRS-1) through caspase-mediated cleavage. J Biol Chem 2007;282:6090–7.

[50] Renström F, Burén J, Eriksson JW. Insulin receptor substrates-1 and -2 are both depleted but via different mechanisms after down-regulation of glucose transport in rat adipocytes. Endocrinology 2005;146:3044–51.
[51] Trayhurn P, Wood IS. Adipokines: inflammation and the pleiotropic role of white adipose tissue. Br J Nutr 2004;92:347–55.
[52] Yin J, Gao Z, He Q, Zhou D, Guo Z, Ye J. Role of hypoxia in obesity-induced disorders of glucose and lipid metabolism in adipose tissue. American Journal of Physiology. Endocrinol Metab 2009;296:E333–42.
[53] Foti DP, Brunetti A. Editorial: "Linking hypoxia to obesity". Front Endocrinol 2017;8:34.
[54] Halberg N, Khan T, Trujillo ME, Wernstedt-Asterholm I, Attie AD, Sherwani S, et al. Hypoxia-inducible factor 1alpha induces fibrosis and insulin resistance in white adipose tissue. Mol Cell Biol 2009;29:4467–83.
[55] Regazzetti C, Peraldi P, Grémeaux T, Najem-Lendom R, Ben-Sahra I, Cormont M, et al. Hypoxia decreases insulin signaling pathways in adipocytes. Diabetes 2009;58:95–103.
[56] Gealekman O, Gurav K, Chouinard M, Straubhaar J, Thompson M, Malkani S, et al. Control of adipose tissue expandability in response to high fat diet by the insulin-like growth factor-binding protein-4. J Biol Chem 2014;289:18327–38.
[57] Nakamura A, Sato K, Kanazawa M, Kondo M, Endo H, Takahashi T, et al. Impact of decreased insulin resistance by ezetimibe on postprandial lipid profiles and endothelial functions in obese, non-diabetic-metabolic syndrome patients with coronary artery disease. Heart Vessels 2019;34:916–25.
[58] Yang Q, Graham TE, Mody N, Preitner F, Peroni OD, Zabolotny JM, et al. Serum retinol binding protein 4 contributes to insulin resistance in obesity and type 2 diabetes. Nature 2005;436:356–62.
[59] Moraes-Vieira PM, Yore MM, Dwyer PM, Syed I, Aryal P, Kahn BB. RBP4 activates antigen-presenting cells, leading to adipose tissue inflammation and systemic insulin resistance. Cell Metab 2014;19:512–26.
[60] Samuel VT, Shulman GI. Mechanisms for insulin resistance: common threads and missing links. Cell 2012;148:852–71.
[61] Knutson VP, Balba Y. 3T3-L1 adipocytes as a cell culture model of insulin resistance. In Vitro Cell Dev Biol: Animal 1997;33:77–81.
[62] Chiefari E, Iiritano S, Paonessa F, Le Pera I, Arcidiacono B, Filocamo M, et al. Pseudogene-mediated posttranscriptional silencing of HMGA1 can result in insulin resistance and type 2 diabetes. Nat Commun 2010;1:40.
[63] Galluzzi L, Vitale I. MiRNAs in aging and cancer. International review of cell and molecular biology, 334. Cambridge, MA, USA: Academic Press; 2017.
[64] Bartel DP. MicroRNAs: genomics, biogenesis, mechanism, and function. Cell 2004;116:281–97.
[65] Eichhorn SW, Guo H, McGeary SE, Rodriguez-Mias RA, Shin C, Baek D, et al. mRNA destabilization is the dominant effect of mammalian microRNAs by the time substantial repression ensues. Mol Cell 2014;56:104–15.
[66] Motohashi N, Alexander MS, Shimizu-Motohashi Y, Myers JA, Genri Kawahara G, Kunkel LM. Regulation of IRS1/Akt insulin signaling by microRNA-128a during myogenesis. J Cell Sci 2013;126:2678–91.
[67] Brunetti A, Foti D, Goldfine ID. Identification of unique nuclear regulatory proteins for the insulin receptor gene, which appear during myocyte and adipocyte differentiation. J Clin Investig 1993;92:1288–95.
[68] Brunetti A, Brunetti L, Foti D, Accili D, Goldfine ID. Human diabetes associated with defects in nuclear regulatory proteins for the insulin receptor gene. J Clin Investig 1996;97:258–62.
[69] Muse ED, Obici S, Bhanot S, Monia BP, McKay RA, Rajala MW, et al. Role of resistin in diet-induced hepatic insulin resistance. J Clin Investig 2004;114:232–9.
[70] Ota T. Chemokine systems link obesity to insulin resistance. Diabetes Metab J 2013;37:165–72.
[71] Laustsen PG, Michael MD, Crute BE, Cohen SE, Ueki K, Kulkarni RN, et al. Lipoatrophic diabetes in Irs1(-/-)/Irs3(-/-) double knockout mice. Genes Dev 2002;16:3213–22.
[72] LeRoith D, Accili D. Mechanisms of disease: using genetically altered mice to study concepts of type 2 diabetes. Nat Clin Pract: Endocrinol Metab 2008;4:164–72.
[73] Graham TE, Yang Q, Blüher M, Hammarstedt A, Ciaraldi TP, Henry RR, et al. Retinol binding protein 4 and insulin resistance in lean, obese, and diabetic subjects. N Engl J Med 2006;354:2552–63.
[74] Trayhurn P, Wang B, Wood IS. Hypoxia in adipose tissue: a basis for the dysregulation of tissue function in obesity? Br J Nutr 2008;100:227–35.
[75] Xiao M, Lou C, Xiao H, Yang Y, Cai X, Li C, et al. MiR-128 regulation of glucose metabolism and cell proliferation in triple-negative breast cancer. Br J Surg 2018;105:75–85.

Update

eBioMedicine

Volume 66, Issue , April 2021, Page

DOI: https://doi.org/10.1016/j.ebiom.2021.103295

EBioMedicine 66 (2021) 103295

Contents lists available at ScienceDirect

EBioMedicine

journal homepage: www.elsevier.com/locate/ebiom

Erratum

Erratum regarding previously published research papers

The following Author Contribution statements were not included in the published versions of the Research Papers that appeared in previous volumes of *EBioMedicine*. The appropriate Author Contribution statements are included below.

Celastrol-induced degradation of FANCD2 sensitises pediatric high-grade gliomas to the DNA-crosslinking agent carboplatin. (*EBioMedicine* **50:** 81–92)

Author contributions: D.S.M. and E.H. conceived and designed the project. D.S.M., M.H.M., P.W. developed and validated the *in vitro* and *in vivo* models used in the study. D.S.M., B.B., M.H.M., and P.W. performed the functional *in vitro* experiments. D.S.M., P.W., and H.M. performed the functional *in vivo* experiments. J.K. provided bioinformatical expertise and support. B.B. and M.H.M., provided material and logistical support and advised on the project. G.J.K. and E.H. acquired funding and supervised the study. All authors contributed to writing the manuscript.

Epigenetically upregulated GEFT-derived invasion and metastasis of rhabdomyosarcoma via epithelial mesenchymal transition promoted by the Rac1/Cdc42-PAK signaling pathway. (*EBioMedicine* **50:** 122–134)

Author contributions: CL and FL designed the whole study and wrote the manuscript. LZ, WC, YP, JD, ZL, QL, HS, LM, WL, YW, YL, PW, YX, YW, LS, JH, and WZ contributed to experimental design and data collection. All authors have agreed with the manuscript and provide their consent for publication.

Combined identification of three miRNAs in serum as effective diagnostic biomarkers for HNSCC. (*EBioMedicine* **50:** 135–143)

Author contributions: CL and QZ conceived the study. ZYY, SYH, and DSZ participated in the study design. QZ and YYJ conducted the study, including acquisition, analysis, and interpretation of data. CL, ZZY, and ZWS drafted the manuscript. All authors critically reviewed, edited, and approved the manuscript and made the decision to submit for publication. All authors assume responsibility for the accuracy and completeness of the data and for the fidelity of the study to the protocol.

Phosphorylated Rasal2 facilitates breast cancer progression. (*EBioMedicine* **50:** 144–55)

Author Contributions: X.W., Y.K. and Z.M.Q. conceived, organized and supervised the study; X.W., M.Y.L. and Y.L.Y.performed the experiments and data collection; Y.L.Y., X.W., C.Q.and K.Y. contributed to the analysis of data and double checking. X.W., C.Q., Y.K., and Z.M.Q. prepared, wrote and revised the manuscript.

Sprouty4 correlates with favorable prognosis in perihilar cholangiocarcinoma by blocking the FGFR-ERK signaling pathway and arresting the cell cycle. (*EBioMedicine* **50:** 166–177)

Author contributions: Q.B, C. TL, S. RQ, L. ZL, Z. XM,and L. ZP carried out experiments. Z.ZL collected the samples. X. YF analysed data. X. YF conceived experiments and wrote the paper. All authors had final approval of the submitted and published versions.

Analysis of gene expression signatures identifies prognostic and functionally distinct ovarian clear cell carcinoma subtypes. (*EBioMedicine* **50:** 203–210)

Author contributions: RYH, TZT, and DSPT, designed and conceptualised the study. DL processed and reviewed OCCC samples. JY performed sample collection and experiments. NYLN curated and reviewed the clinical data of NUH cohort. TZT performed bioinformatics analyses. RYH, TZT, CVY, NYLN and DSPT analysed the data, interpret the results, and wrote the manuscript.

Pro-inflammatory monocyte profile in patients with Major Depressive Disorder and suicide behavior and how ketamine induces anti-inflammatory M2 macrophages by NMDAR and mTOR. (*EBioMedicine* **50:** 290–305)

DOI of original article: http://dx.doi.org/10.1016/j.ebiom.2019.10.060, http://dx.doi.org/10.1016/j.ebiom.2019.11.016, http://dx.doi.org/10.1016/j.ebiom.2019.11.017, http://dx.doi.org/10.1016/j.ebiom.2019.11.027, http://dx.doi.org/10.1016/j.ebiom.2019.11.028, http://dx.doi.org/10.1016/j.ebiom.2019.11.047, http://dx.doi.org/10.1016/j.ebiom.2020.102632, http://dx.doi.org/10.1016/j.ebiom.2020.102659, http://dx.doi.org/10.1016/j.ebiom.2020.102664, http://dx.doi.org/10.1016/j.ebiom.2020.102740, http://dx.doi.org/10.1016/j.ebiom.2020.102763, http://dx.doi.org/10.1016/j.ebiom.2020.102891, http://dx.doi.org/10.1016/j.ebiom.2020.102631, http://dx.doi.org/10.1016/j.ebiom.2020.102723, http://dx.doi.org/10.1016/j.ebiom.2020.102730, http://dx.doi.org/10.1016/j.ebiom.2020.102766, http://dx.doi.org/10.1016/j.ebiom.2020.102831, http://dx.doi.org/10.1016/j.ebiom.2020.102895, http://dx.doi.org/10.1016/j.ebiom.2019.11.010, http://dx.doi.org/10.1016/j.ebiom.2019.102597, http://dx.doi.org/10.1016/j.ebiom.2019.102615, http://dx.doi.org/10.1016/j.ebiom.2020.102660, http://dx.doi.org/10.1016/j.ebiom.2020.102724, http://dx.doi.org/10.1016/j.ebiom.2020.102733, http://dx.doi.org/10.1016/j.ebiom.2020.102742, http://dx.doi.org/10.1016/j.ebiom.2020.102747, http://dx.doi.org/10.1016/j.ebiom.2020.102783, http://dx.doi.org/10.1016/j.ebiom.2020.102838, http://dx.doi.org/10.1016/j.ebiom.2019.10.062, http://dx.doi.org/10.1016/j.ebiom.2019.11.039, http://dx.doi.org/10.1016/j.ebiom.2019.11.044, http://dx.doi.org/10.1016/j.ebiom.2019.102611, http://dx.doi.org/10.1016/j.ebiom.2020.102640, http://dx.doi.org/10.1016/j.ebiom.2020.102657, http://dx.doi.org/10.1016/j.ebiom.2020.102728, http://dx.doi.org/10.1016/j.ebiom.2020.102803, http://dx.doi.org/10.1016/j.ebiom.2020.102842, http://dx.doi.org/10.1016/j.ebiom.2019.11.019, http://dx.doi.org/10.1016/j.ebiom.2019.10.063, http://dx.doi.org/10.1016/j.ebiom.2019.11.042, http://dx.doi.org/10.1016/j.ebiom.2019.11.045, http://dx.doi.org/10.1016/j.ebiom.2019.102599, http://dx.doi.org/10.1016/j.ebiom.2019.102622, http://dx.doi.org/10.1016/j.ebiom.2020.102860, http://dx.doi.org/10.1016/j.ebiom.2020.102912, http://dx.doi.org/10.1016/j.ebiom.2019.11.021, http://dx.doi.org/10.1016/j.ebiom.2019.11.022, http://dx.doi.org/10.1016/j.ebiom.2020.102685, http://dx.doi.org/10.1016/j.ebiom.2020.102693, http://dx.doi.org/10.1016/j.ebiom.2020.102695, http://dx.doi.org/10.1016/j.ebiom.2020.102710, http://dx.doi.org/10.1016/j.ebiom.2020.102722, http://dx.doi.org/10.1016/j.ebiom.2020.102748, http://dx.doi.org/10.1016/j.ebiom.2020.102767, http://dx.doi.org/10.1016/j.ebiom.2020.102807, http://dx.doi.org/10.1016/j.ebiom.2020.102883, http://dx.doi.org/10.1016/j.ebiom.2020.102674, http://dx.doi.org/10.1016/j.ebiom.2020.102683, http://dx.doi.org/10.1016/j.ebiom.2020.102759, http://dx.doi.org/10.1016/j.ebiom.2020.102843, http://dx.doi.org/10.1016/j.ebiom.2019.11.032, http://dx.doi.org/10.1016/j.ebiom.2019.102598, http://dx.doi.org/10.1016/j.ebiom.2019.102602, http://dx.doi.org/10.1016/j.ebiom.2019.102621, http://dx.doi.org/10.1016/j.ebiom.2020.102656, http://dx.doi.org/10.1016/j.ebiom.2020.102679, http://dx.doi.org/10.1016/j.ebiom.2020.102689, http://dx.doi.org/10.1016/j.ebiom.2020.102738, http://dx.doi.org/10.1016/j.ebiom.2020.102750.

https://doi.org/10.1016/j.ebiom.2021.103295
2352-3964/© 2021 The Author(s). Published by Elsevier B.V. All rights reserved

Author contributions: W.N. designed and performed *in vitro* experiments, analysed and discussed results, and critically revised the manuscript. L.N.G. and D.E.R. recruited and followed up patients with MDD and performed sample collection. I.G.E. and N.E. performed *in vitro* experiments. A.R.A. processed samples of patients with MDD. M.P.A. and L.M.S. designed and performed *in vivo* murine experiments, analysed and discussed results, and critically revised the manuscript. F.M.D. conceived and designed the study, recruited and followed up patients with MDD, discussed results, and wrote the manuscript. E.A.C.S. and A.E.E. conceived and designed the study, designed and performed experiments, analysed and discussed results, and wrote the manuscript.

Radiomics analysis of placenta on T2WI facilitates prediction of postpartum hemorrhage: A multicentre study. (*EBioMedicine* **50:** 355–365)

Author Contributions: Conception and design: Xiaoan Zhang, Jie Tian, Meiyun Wang. Collection and assembly of data: Qingxia Wu, Kuan Yao, Zhenyu Liu, Longfei Li, Xin Zhao, Shuo Wang, Honglei Shang, Yusong Lin, Zejun Wen. Development of methodology: Kuan Yao, Zhenyu Liu, Longfei Li, Shuo Wang, Yusong Lin, Jie Tian. Data analysis and interpretation: All authors. Manuscript writing: All authors. Final approval of manuscript: All authors.

TP63 Isoform Expression is Linked with Distinct Clinical Outcomes in Cancer. (*EBioMedicine* **51:** 102,561)

Author contributions: A.B. designed experiments, analyzed data and wrote the manuscript. T.M. performed PCR and RT-PCR experiments. Y.W. performed western blot validation experiments. P.B. contributed to statistical design and analysis of data. P.P. supervised experimental design, analyzed data and prepared the manuscript. All authors read and approved of final manuscript.

Serum IGFBP-1 as a potential biomarker for diagnosis of early-stage upper gastrointestinal tumor. (*EBioMedicine* **51:** 102,566)

Author contributions: Y-WX designed the study, searched the literature, performed the experiments, analysed and interpreted the data, did the statistical analysis, and wrote the manuscript. HC designed the study, collected patient samples, performed the experiments, analysed, and interpreted the data. C-QH designed the study, collected patient samples, searched the literature, did the statistical analysis, analysed, and interpreted the data. L-YC collected patient samples, performed the experiments, analysed and interpreted the data. S-HY analysed and interpreted the data. L-SH, and HG collected patient samples and clinical data. L-YC, C-TL, X-YH L-HL and S-LC collected patient samples and clinical data. Z-YW, Y-HP, L-YX, and E-ML conceptualized and designed the study, supervised the project, and revised the paper. All authors vouch for the respective data and analysis, and agreed to publish the manuscript.

Diagnostic accuracy and easy applicability of intestinal auto-antibodies in the wide clinical spectrum of coeliac disease. (*EBioMedicine* **51:** 102,567)

Author contributions: Study concept and design: Luigina De Leo, Tarcisio Not. Acquisition of data: Luigina De Leo, Stefano Martelossi, Grazie Di Leo, Matteo Bramuzzo. Analysis and interpretation of data: Luigina De Leo, Tarcisio Not, Stefano Martelossi, Grazia Di Leo, Matteo Bramuzzo, Vincenzo Villanacci, Chiara Zanchi. Drafting of the manuscript: Tarcisio Not, Luigina De Leo. Critical revision of the manuscript: Alessandro Ventura, Vincenzo Villanacci, Matteo Bramuzzo, Chiara Zanchi. Clinical decisions: Stefano Martelossi, Grazie Di Leo, Matteo Bramuzzo. Histological evaluation of biopsy samples: Vincenzo Villanacci. Intestinal antibodies immunoassays: Luigina De Leo, Michela Pandullo, Petra Riznik

Phage display antibody libraries: Fabiana Ziberna. Statistical analysis: Fabiola Giudici. All authors read and approved the final version of the manuscript.

MEF2C Repressor Variant Deregulation Leads To Cell Cycle Re-Entry and Development of Heart Failure. (*EBioMedicine* **51:** 102,571)

Author contributions: AHMP, ACC designed and performed experiments, analyzed data, and wrote the manuscript. SRC, RRO, AS an MLBV designed and performed experiments. JRMS performed the echocardiography in animals. MFC analyzed data. AG, JLF, GCAR and MML provided human samples. JDM discussed the manuscript. KGF designed experiments, analyzed data, and wrote the manuscript. All authors reviewed and commented on the manuscript.

Developments in Zebrafish Avatars as radiotherapy sensitivity reporters – towards personalized medicine. (*EBioMedicine* **51:** 102,578)

Author contributions: R.F. and M.G.F. conceptualized the research; R.F. and B.C. supervised the research; S.F., B.C., V.P and R.F. performed research, acquisition, analysis and interpretation of data; P.F., R.R-T., N.F. provided primary tumor samples; M.J.C, S.V., J.S., performed calculations and set-up the accelerator, O.P., J.S. for fruitful discussions; R.F. and B.C. wrote the manuscript. S.F., C.G., O.P. and M. G.F. did critical reading and editing of the manuscript.

Multi-cancer V-ATPase molecular signatures: A distinctive balance of subunit *C* isoforms in esophageal carcinoma. (*EBioMedicine* **51:** 102,581)

Author contributions: JCVCS performed most of the experiments and analysis. PNN participated in the analysis and acquisition of data. EPC performed the in silico structural models. ARF and LFRP coordinated the project. JCVCS and ARF wrote the manuscript. JCVCS, PNN, TAS, ARF and LFRP performed study design. TAS and PNN participated in the collection of samples. ALOF and FFF provided specialized scientific and technical support. All authors discussed the results and manuscript text. All authors read and approved the final manuscript.

Heterogeneous nuclear ribonucleoprotein A2/B1 is a negative regulator of human breast cancer metastasis by maintaining the balance of multiple genes and pathways. (*EBioMedicine* **51:** 102,583)

Author Contributions: The authors' work in this study is listed as follows: *In vitro* and *in vivo* assays (YL, HL, FL, LBG, RH, CC and XD); RNA immunoprecipitation (YL); dual-luciferase reporter assay (YL and SL), signal pathways analysis (HL), proteomic analysis (YL), EMT markers test (HL, LBG and RH); real-time PCR (YL, SL, KL, LY, HMT, BBC and XL); and tissue microarray analysis (YL, DHX and XLD). SLS designed and supervised the study. YL and SLS analysed data and wrote manuscripts.

Genetic Risk for Dengue Hemorrhagic Fever and Dengue Fever in Multiple Ancestries. (*EBioMedicine* **51:** 102,584)

Author contributions: GP, ML, KH, IL contributed to the design; ML, SE, LG, GK, AB, IL, LP, CP, IF, RS, ED, FB, YR, PB, JN, LW, DS, SP, GP, AW, CR, LP acquisition of data; GP, ML, AB, LG, GK Interpretation of data; GP, ML, PS, IL drafted the manuscript; IF, LW, DS, SP, GP, AW, AB, ED, LG, GK, ML, RS, KH revised it for critical intellectual content; ML, SE, LG, GK, AB, IL, LP, CP, IF, RS, ED, FB, YR, PB, JN, LW, DS, SP, GP, AW, PS, GK, KH approved the final manuscript; PG, ML, PS, SE, IF, LW, DS, SP, GP, AW, JN, AB, ED, LG, GK, RS, KH agree to be accountable for all aspects of the work.

Cortical haemodynamic response measured by functional near infrared spectroscopy during a verbal fluency task in patients with major depression and borderline personality disorder. (*EBioMedicine* **51:** 102,586)

Author contributions: Syeda F. Husain: Formal analysis, Investigation, Methodology, Visualization, Writing – original draft, Writing-review & editing. Tong-Boon Tang: Supervision, Writing - review & editing. Rongjun Yu: Supervision, Writing - review & editing. Wilson W. Tam: Supervision, Methodology, Writing - review & editing. Bach Tran: Supervision, Writing - review & editing. Travis T. Quek: Participant recruitment, Writing – review & editing. Shi-Hui Hwang: Participant recruitment, Writing – review & editing. Cheryl W. Chang: Participant recruitment, Writing – review & editing. Cyrus S. Ho: Supervision, Writing - review & editing. Roger C. Ho: Conceptualisation, Participant Recruitment, Methodology, Writing – review & editing.

Impact of sitagliptin on endometrial mesenchymal stem-like progenitor cells: A randomised, double-blind placebo-controlled feasibility trial. (*EBioMedicine* **51:** 102,597)

Author contributions: Study concept, design, and overall supervision: J.J.B, S.Q. Prepared manuscript: J.J.B., S.Te., E.S.L., S.Q. Edited manuscript: L.L., L.J.E., M.J.M.D.C., K.J.F., J.M., P.J.B., A.P., P.K.K., R.F. Obtained funding: S.Q., J.J.B, S.Ta. Regulatory approvals: S.Q., S.Te. Patient enrolment, consenting, ultrasound and clinical assessments: S.Q., S.Te., A.P., L.J.E., L.L. CFU assays and analysis: E.S.L., P.J.B. Exploratory investigations: E.S.L., R.F., P.J.B, J.M., K.J.F., M.J.M.D.C., J.J.B. Data analysis: P.K.K., E.S.L., S.Te., J.J.B., S.Q.

The CD24+ Cell Subset Promotes Invasion and Metastasis in Human Osteosarcoma. (*EBioMedicine* **51:** 102,598)

Author contributions: Zhenhua Zhou wrote the manuscript. Zhenhua Zhou, Yan Li and Muyu Kuang performed cell culture, real-time PCR, flow cytometry and animal experiments. Xudong Wang carried out cell migration, invasion, proliferation assays, Western blot and protein mass spectrometry. Jingjing Hu and Jiashi Cao carried out the histological analysis and scores evaluation. Qi Jia and Sujia Wu carried out prognosis statistical analysis of clinical cases. Zhiwei Wang and Jianru Xiao conceived of the study and participated in its designation and helped to draft the manuscript. All authors read and approved the final manuscript.

The Transferability and Evolution of NDM-1 and KPC-2 co-producing Klebsiella pneumoniae from Clinical Settings. (*EBioMedicine* **51:** 102,599)

Author contributions: HW conceived the project and designed the experiments. QW collected samples and performed microbial identification. YL collected the medical records. RW, YL and LJ performed the microbiological experiments. HG performed the computational analyses. YL, HG, RW and HW wrote the manuscript. All authors read and commented on successive drafts and all approved the content of the final version. tumor immune cell infiltration and survival after platinum-based chemotherapy in high-grade serous ovarian cancer subtypes: A gene expression-based computational study. (*EBioMedicine* **51:** 102,602)

Author contributions: RL, WZ and HHZ contributed to the study design. YZ and RH contributed to data collection. RL performed statistical analysis, interpretation and drafted the manuscript. All authors contributed to critical revision of the final manuscript. RL approved the final version of the manuscript.

Mucosal microbial load in Crohn's disease: a potential predictor of response to fecal microbiota transplantation. (*EBioMedicine* **51:** 102,611)

Author contributions: C.M. and G.S. conceived and supervised the study. G.S., E.V., D.C., A.S, J.W. performed the experiments and data analysis. M.P. and C.M. performed the 16S rRNA data analysis and interpretation. S.L., M.M. and E.E. provided the explant tissues and reviewed the manuscript. C.E. provided the patients' clinical data. K.M. and S.V. provided the mucosal biopsies from CD patients and reviewed the manuscript. G.S. and C.M. wrote and reviewed the manuscript. A.C. revised the manuscript. All authors read and approved the final version of the manuscript.

Mesenchymal stem cells ameliorate β cell dysfunction of human type 2 diabetic islets by reversing β cell dedifferentiation. (*EBioMedicine* **51:** 102,615)

Author contributions: Conceptualization, Z.S., S.W.; Funding acquisition, Z.S., S.W.; Study design, L.W., T.L., R.L.; Investigation, L. W., T.L., R.L.; Data analysis, L.W., T.L., R.L.; Methodology, L.W., T.L., G. W., R.L., N.L., B.Z., Y.J.L., X.D., X.C., Y.L.; Data interpretation, S.W., Z.S., Z.W., X.X.; Supervision, S.W., Z.S., C.R.; Writing – original draft, R.L., L. W; Writing – review & editing, Z.S., S.W., X.X., C.R..

A practical model for the identification of congenital cataracts using machine learning. (*EBioMedicine* **51:** 102,621)

Author Contributions: HL, DL, WC, and YL contributed to the concept of the study and critically reviewed the manuscript. HL, DL, JC, ZL, YX, and XL designed the study and performed the literature search. HL, DL, JC, ZL, XL, XW, ZL, and WC collected the data. KZ, JH, LZ, and CG contributed to the design of the statistical analysis plan. DL, KZ, and JLH performed the data analysis and data interpretation. DL and HL drafted the manuscript. HL, DL, CC, YX, LW, and YZ critically revised the manuscript. HL, DL, WC, and YL provided research funding, coordinated the research and oversaw the project. All authors reviewed the manuscript for important intellectual content and approved the final manuscript.

MiR-765 functions as a tumor suppressor and eliminates lipids in clear cell renal cell carcinoma by downregulating PLP2. (*EBioMedicine* **51:** 102,622)

Author contributions: WX, CW and XPZ designed and performed the experiments. WX, JCX and CW wrote the manuscript. WX, KC and TW analyzed and performed the experiments. XGW and XPZ directed the experiments and analyzed and assembled the data. All authors read and approved the submitted manuscript.

Breast cancer induces systemic immune changes on cytokine signaling in peripheral blood monocytes and lymphocytes. (*EBioMedicine* **51:** 102,631)

Author contributions: LW and PPL designed experiments; LW, DLS, TYT and CA conducted experiments; LW and XL analyzed experimental data; AYC, FMD, JY, JW identified and recruited patients into this study; LW and PPL wrote manuscript. All authors read and approved the manuscript.

Near Infrared Photoimmunotherapy Targeting DLL3 For Small Cell Lung Cancer. (*EBioMedicine* **51:** 102,632)

Author contributions: The all authors checked and approved the final version of the manuscript. Y.I. and K.S. mainly conducted all experiments, performed analysis and wrote the manuscript; K.T., S.T., H.Y., Y.N., R.E., M.S., C.K., N.K., H.Y., Y.B., and Y.H. conducted analysis; S.N., T.F., K.K. and T.F.C.Y. conducted surgical operation to gather the specimens; K.S. supervised and conducted the project.

Gut microbiota composition during infancy and subsequent behavioural outcomes. (*EBioMedicine* **51:** 102,640)

Author contributions: AL and PV proposed the analysis. AL, MOH, ALP, and FC contributed to the statistical analysis. AL, PV, ALP, MOH, CS, FC, and MT contributed to data interpretation. FC contributed to biobanking. AL, PV, and MOH drafted the manuscript. All authors provided feedback and edits to the manuscript. Relevant grant funding applications were prepared by and awarded to: PV, ALP, JC, CS, FC, MT, SR, KA, RS, LH, PS, and the BIS Investigator Group.

Intracavernous injection of size-specific stem cell spheroids for neurogenic erectile dysfunction: efficacy and risk versus single cells. (*EBioMedicine* **52:** 102,656)

Author contributions: ZQL and YT designed the whole experiments and guided the entire experiments, and are responsible for the integrity of the data and the accuracy of the data analysis; YDX and ZQL contributed to performance the animal experiments, data analysis and manuscript drafting. HZ, CH, XMZ, YCZ, and RLG contributed to the performance of the experiments. ZCX and ZQL analyzed and interpreted the data, and critically revised the manuscript for important intellectual content. All authors approved the final version of the manuscript.

Identification and external validation of IgA nephropathy patients benefiting from immunosuppression therapy. (*EBioMedicine* **52:** 102,657)

Authors contributions: Research idea and study design: Z-HL, G-TX, C-HZ, T-YC, E-YX, T-GC; data acquisition: Z-HL, C-HZ, T-YC, E-YX, T-GC, XL; data analysis/interpretation: Z-HL, C-HZ, T-YC, E-YX, T-GC, XL, YZ; statistical analysis: T-YC, E-YX,T-GC,YZ; supervision or mentorship: Z-HL, C-HZ, YQ, S-SL, FX, D-DL. All authors read and approved the final version of the manuscript.

Classification of Primary Liver Cancer with Immunosuppression Mechanisms and Correlation with Genomic Alterations. .(*EBioMedicine* **52:** 102,659)

Authors contributions: H.N. conceived the study. M.F., R.Y., T.H, S.H., and K.K. performed the analysis. K.M., K.N., A.F., M.U., S.H., H.A., H.Y., K.C., and S.I. contributed materials and data. K.A. performed immunohistochemical analysis. S.S. and S.T. performed cell line experiments and expression analysis. H.T. and S.M. contributed to the supercomputer environment. M.F. and H.N. wrote the manuscript.

Silencing of circular RNA HIPK2 in neural stem cells enhances functional recovery following ischaemic stroke. (*EBioMedicine* **52:** 102,660)

Author contributions: H.Y. conceived and supervised this project. H.Y and G.W. designed the experiments. G.W., B.H., L.S., S.W., L.Y., J.L., F.W., M.L., S.L., F.Z., Y.Z., Y.B., Y.M. and B.C. conducted experiments and acquired, analysed and interpreted the data. H.Y. and G.W. wrote the manuscript. All authors read and approved the final version of the manuscript.

Genome-wide identification of FHL1 as a powerful prognostic candidate and potential therapeutic target in acute myeloid leukaemia. (*EBioMedicine* **52:** 102,664)

Author contributions: CC and YF designed the study. YF, MX, ZC performed the experiments. YF, ZY, ZZ, XY and XH analyzed the data. CC, MZ and XW obtained the funding. YF, MX, MZ and XW prepared the figures. YF, MX, ZC and CC wrote the manuscript. CC supervised the study. All authors read and approved the final manuscript.

Longitudinal Serum Autoantibody Repertoire Profiling Identifies Surgery-Associated Biomarkers in Lung Adenocarcinoma. (*EBioMedicine* **52:** 102,674)

Author contributions: S-C. T. and H-C. L. developed the conceptual ideas and designed the study. Y. L, S-J. G., H-W. J. performed the experiments, C-Q. L. and W. G. collected the sera samples. S-C.T., H-C. L., Y. L. and C-Q. L. wrote the manuscript with suggestions from the other authors.

A comprehensive analysis of candidate genes in familial pancreatic cancer families reveals a high frequency of potentially pathogenic germline variants. (*EBioMedicine* **53:** 102,675)

Author contributions: Study design: JE, NM and AC. Data collection: JE, MEC, VP, RF, MRG, TRA, LRD, ICG, MR, EMC and MM. Experimental work: JE, CG, JE2, EB, SGM, DG, GM. Data Analysis: JE, JE2, EB, DG, GM and JR. Interpretation of the data: JE, VP, RF, TRA, LRD, ICG, MR, EMC, NM and AC. Preparation of the manuscript: all authors

CircRNA-CIDN mitigated compression loading-induced damage in human nucleus pulposus cells via miR-34a-5p/SIRT1 axis. (*EBioMedicine* **53:** 102,679)

Author Contributions: Q.X. and L.K. designed the study protocol and wrote the manuscript; Q.X., L.K. and J.W. conducted the experiments; Z.L. and Y.S. established the ex vivo IVD cultured model; K.Z. and K.W. collected and analysed data; C.Y. collected the NP tissues and supervised the study; Y.Z. supported and supervised the study.

FGFR1 and FGFR4 oncogenicity depends on N-Cadherin and their co-expression may predict FGFR-targeted therapy efficacy. (*EBioMedicine* **53:** 102,683)

Author contributions: Conceptualization: A.Q., I.F., S.M.P., A.C., and L.P.A.; Methodology: A.Q., A.C., S.V.C, I.F., and S.M.P.; Investigation: A.Q., A.C., I.F., S.V.C., L.P.A. and S.M.P.; Validation: A.Q.,A.M., L.O., E.G., S.V.C, S.M.G, L.M, S.G. and F.L.R.; Formal Analysis: A.Q., I.F., J.Z., S. M.P; Writing – Original Draft: A.Q., I.F., A.C., S.M.P. and L.P.A., Writing – Review & Editing: A.Q., I.F., S.V.C, A.C., S.M.P. and L.P.A., Supervision: A.C., I.F., S.M.P., and L.P.A.; Funding Acquisition: S.M.P., I.F. and L.P.A. All authors read and approved the final version of the manuscript.

BAP18 is involved in upregulation of CCND1/2 transcription to promote cell growth in oral squamous cell carcinoma. (*EBioMedicine* **53:** 102,685)

Author contributions: Xue Wang, Chunyu Wang, and Guangqi Yan designed the study and wrote the manuscript, Xue Wang, Ge Sun, Yuanyuan Kang, Shengli Wang, Renlong Zou, Hongmiao Sun and Kai Zeng performed experiments and analyzed the data, Huijuan Song, Wei Liu, Ning Sun, and Wensu Liu conducted bioinformatic analyses and statistical analyses, Yue Zhao wrote and revised manuscript. All authors read the approved the final manuscript.

Systematic identification of CDC34 that functions to stabilize EGFR and promote lung carcinogenesis. (*EBioMedicine* **53:** 102,689)

Author Contributions: The project was conceived and designed by G.B.Z. The experiments were conducted by X.C.Z, G.Z.W., Q.H., L. W.Q., S.H.G., J.L., L.M., Y.F.Z., C.Z., H.Y., D.L.Z., and M.W.. Biospecimens were harvested/provided by Z.S.W., Y.C.Z., Y.C.H., B.Z., C.L.W., and Z.L.. The EGFR transgenic mice were provided by L.C.. Data were analyzed by G.B.Z., Y.Z., Z.L., L.C., and X.C.Z.. The manuscript was written by G. B.Z.. The study sponsor had no role in the design of the study; the data collection, analysis, or interpretation; the writing of the article; or the decision to submit for publication.

CBX4 transcriptionally suppresses KLF6 via interaction with HDAC1 to exert oncogenic activities in clear cell renal cell carcinoma. (*EBioMedicine* **53:** 102,692)

Author contributions: Conception and design of the study: Jiang N, Zhang CZ, Shen HM; Generation, collection, assembly, analysis of data: Jiang N, Niu G, Pan YH, Pan WW, Zhang MF; Drafting and revision of the manuscript: Jiang N, Zhang CZ, Shen HM; Approval of the final version of the manuscript: all authors.

Enhanced O-linked GlcNAcylation in Crohn's disease promotes intestinal inflammation. (*EBioMedicine* **53:** 102,693)

Author contributions: Q.H.S. wrote the manuscript. Z.X.X. contributed to the conception and writing. W.Y.S., Y.L.L., and Z.X.X. designed research; Q.H.S., Y.P.J., M.D.L., D.Z., R.X.Z., J.C., and Y.L., performed research; C.S.Q., Y.S.W., G.L., H.L.Z., Q.D., J.L., Y.L.L., and Z.X.X. analyzed the data. Q.H.S., G.L., H.L.Z., Q.D., and Z.X.X. revised the manuscript. All authors read and approved the final manuscript.

Elevated myocardial SORBS2 and the underlying implications in left ventricular noncompaction cardiomyopathy. (*EBioMedicine* **53:** 102,695)

Author contributions: Yingjie Wei. supervised the work; Yingjie Wei, Chunyan Li. designed the experiments with help from Fan Liu, Shenghua Liu, Haizhou Pan, Haiwei Du, Jian Huang, Yuanyuan Xie, Yanfen Li and Ranxu Zhao. Yingjie Wei, Chunyan Li and Fan Liu analyzed the data; Chunyan Li and Yingjie Wei cowrote the manuscript. All authors discussed the results and commented on the manuscript.

Artificial intelligence-assisted prediction of preeclampsia: development and external validation of a nationwide health insurance dataset of the BPJS Kesehatan in Indonesia. (*EBioMedicine* **54:** 102,710)

Author contributions: HS and ECYS developed the concept and design of this study. Dataset access was requested by HS. This author and YWW, and ECYS had full access to all data in the study. HS extracted and processed the data, performed training and validation of machine learning algorithms, conducted the literature search and wrote the draft of the manuscript. HS, YWW, and ECYS independently assessed the eligibility criteria of reviewed studies. YWW and ECYS critically revised the drafted manuscript. HS and ECYS take responsibility for data integrity and the accuracy of the analysis. All authors reviewed the final manuscript.

Plantar temperatures in stance position: A comparative study with healthy volunteers and diabetes patients diagnosed with sensoric neuropathy. (*EBioMedicine* **54:** 102,712)

Author Contributions: UN, MS, JM, AM and PRM contributed equally to this study. PRM and SK conceived and designed the study. ED, JK, SK, JM, AM, and IW recruited participants and performed the experiments. UN, MS, JM, AM and PRM analyzed the data. UN, MS, JM, and PRM drafted the manuscript. TS and PRM were responsible for the design and performance of the sensor-equipped insoles and for data retrieval.

TRAF4 acts as a fate checkpoint to regulate the adipogenic differentiation of MSCs by activating PKM2. (*EBioMedicine* **54:** 102,722)

Author contributions: SC, JL, ZC and YP designed the study and performed the experiments. ZS, ZL and GY performed the statistical analyses. GZ, ML, WL, WY and SW contributed study material and reagents. SC, ZX, PW and HS wrote the manuscript. ZX, PW and HS are the corresponding authors. All authors read and approved the final manuscript.

Identification, clinical manifestation and structural mechanisms of mutations in AMPK associated cardiac glycogen storage disease. (*EBioMedicine* **54:** 102,723)

Author Contributions: Dan.H, and Dong.H. designed the study. Dong.H., H.B.M, L.W.L., N.B.S., Y.L., B.W., F.Z., B.L.S., A.A., L.M., Y.X., S. W., C.A., M.H.G., P.M.E., Dan.H performed clinical and pathological phenotyping of study subjects. Dan.H, H.B.M, and Dong.H. coordinated the clinical evaluations. Dan.H, H.B.M, M.H.G., P.M.E., and Dong. H. supervised and coordinated the genetic laboratory work. Y.L., Y.X., S.W., Dan.H, and D.B., performed history analysis. H.M., K.M., K.L., Dan.H, and D.B., performed computational modeling calculations and transfer entropy analysis. Dan.H, H.B.M, and Dong.H. organized and summarized the database. Dan.H, H.B.M, L.W.L., D,B. and Dong.H. analyzed the data. Dan.H, D,B. C.A., M.H.G., P.M.E., and Dong.H. developed the conceptual approaches to data analysis. Dan.H, Dong.H. D,B. and H.B.M, wrote the manuscript. All co-authors contributed to critical editing of manuscript.

Precise pulmonary scanning and reducing medical radiation exposure by developing a clinically applicable intelligent CT system: Toward improving patient care. (*EBioMedicine* **54:** 102,724)

Author contributions: Conceptualization: Yang Wang and Bing Zhang; Experimental and data studies: Yang Wang, Xiaofan Lu, Yingwei Zhang, Xin Zhang, Kun Wang, Jiani Liu, and Xin Li; Technical Support: Renfang Hu, Xiaolin Meng, Shidan Dou, Huayin Hao, Xiaofen Zhao, Wei Hu, Cheng Li, and Yaozong Gao; Statistical analysis: Xiaofan Lu and Fangrong Yan; Construction of artificial intelligence network: Renfang Hu, Xiaolin Meng, Shidan Dou, Huayin Hao, Xiaofen Zhao, Wei Hu, Cheng Li, and Yaozong Gao; Manuscript editing: Yang Wang, Xiaofan Lu, Zhishun Wang, Guangming Lu, Fangrong Yan, and Bing Zhang; Funding acquistion: Fangrong Yan and Bing Zhang; Resources: Fangrong Yan and Bing Zhang; Supervision: Fangrong Yan and Bing Zhang. All authors read and approved the final version of the manuscript.

Clinical and genomic insights into circulating tumor DNA-based alterations across the spectrum of metastatic hormone-sensitive and castrate-resistant prostate cancer. (*EBioMedicine* **54:** 102,728)

Author Contributions: Conception of idea, MK; Acquisition of data, MK, WT, LH, KM, HF, EK, AA, SY; Data generation, AW, CM, CW; Analysis and interpretation of data, TZ, JY, MK, AW, CM, CW, PD, HF, EK, AA; Drafting of the manuscript, MK, AA, TZ, JY, WT; Critical revision of the manuscript for important intellectual data, WT, LH, SJ, KM, JY, TZ, SJ, HF, SY, EK, AA; Obtaining funding, MK, LH, AA, EK, KM.

Lifetime risk of autosomal recessive mitochondrial disorders calculated from genetic databases. (*EBioMedicine* **54:** 102,730)

Author contributions: MW and TK conceived the study. JT and MW defined a comprehensive list of mitochondrial disease genes and set up a list of pathogenic variants in these genes, supported by SLS, TMS, and SBW. JT and MW queried two databases (gnomAD and in house) to assess the allele frequencies of disease-causing variants in the general population and calculated the lifetime risks, supported by HP, TM, KO and TK. JT and MW drafted the manuscript which was then refined by all other authors and finalized by MW and TK.

Transcriptional and clonal characterization of B cell plasmablast diversity following primary and secondary natural DENV infection. (*EBioMedicine* **54:** 102,733)

Author contributions: A.T.W conceived of the project, designed and executed experiments, analyzed data, and wrote the paper. G.G. and W.R. designed and executed experiments, analyzed data, and provided subject matter expertise. M.K.M. and B.G. analyzed data. T.L., H.S., K.V., C.K., A.G., M.E.F., and J.L. generated data. A.M, A.S., E.D., S.F. provided subject matter expertise and supervised data generation. B.J.D. secured funding. T.E., S.T., and A.L.R. secured funding and provided subject matter expertise. R.G.J. provided project oversight, secured funding, and provided subject matter expertise. D.E. provided project oversight and subject matter expertise. J.R.C and H.F. conceived of the project, designed and executed experiments and analyzed data.

Zika Virus Envelope Nanoparticle Antibodies Protect Mice without Risk of Disease Enhancement. (*EBioMedicine* **54:** 102,738)

Author contributions: Literature search: SS; Figures: RS, RKS, SS, NK; Study design: SS, NK, JKL, FK; Data collection: RS, RKS, VR, UA, GB, JAA; Data analysis and interpretation: SS, NK, JKL, FK; Writing: SS and NK; Approval of final manuscript: all authors.

Bio responsive self-assembly of Au-miRNAs for targeted cancer theranostics. (*EBioMedicine* **54:** 102,740)

Author contributions: The authors' responsibilities were as follows: WC, LY, YW and XW devised the experiments and wrote the manuscript. WC conducted the synthesis of materials, purification, and materials/biological characterizations etc. HF contributed to the mouse model experiment. All other authors contributed to materials synthesis, purification/characterization, and/or discussion of the results.

Large-scale network dysfunction in the acute state compared to the remitted state of bipolar disorder: A meta-analysis of resting-state functional connectivity. (*EBioMedicine* **54:** 102,742)

Author Contributions: Yanlin Wang and Xiaoqi Huang designed the study, Yanlin Wang and Shi Tang collected data and performed analyses; Lu Lu, Lianqing Zhang, Xinyu Hu, Xuan Bu, Hailong Li, Xiaoxiao Hu, Xinyu Hu, Ping Jiang, and Zhiyun Jia provided helpful suggestions; Yanlin Wang, Yingxue Gao and Shi Tang drafted the main article; John A. Sweeney, Qiyong Gong and Xiaoqi Huang critically reviewed the manuscript.

Dynamics of within-host Mycobacterium tuberculosis diversity and heteroresistance during treatment. (*EBioMedicine* **55:** 102,747)

Author contributions: Study design: CN, JB, FB; Data collection: CN, KB, JM, AG, NP, MO; Data analysis: CN, FB; Data interpretation: CN, JM, MO, FB; Writing: CN, FB; Review and approval of manuscript: CN, KB, JM, AG, NP, MO, JB, FB; All authors have read and approved the final version of this manuscript.

Host transcriptomic signature as alternative test-of-cure in visceral leishmaniasis patients coinfected with HIV. (*EBioMedicine* **55:** 102,748)

Author contributions: All authors read and approved the final version of the manuscript. Wim Adriaensen: Conceptualization, data curation, formal analysis, investigation, visualization, writing & editing Bart Cuypers: Formal analysis, methodology, writing, review & editing Carlota F. Cordero: Formal analysis Bewketu Mengasha: Data collection and curation Séverine Blesson: Data curation, project coordination Lieselotte Cnops: Formal analysis, writing, review & editing Paul M. Kaye: Methodology, supervision, review & editing Fabiana Alves: Data curation, funding acquisition, project administration, review & editing Ermias Diro: Data curation, project coordination, funding acquisition, review & editing Johan van Griensven: Conceptualization, methodology, funding acquisition, project administration, supervision, review & editing

Motor transmission defects with sex differences in a new mouse model of mild spinal muscular atrophy. (*EBioMedicine* **55:** 102,750)

Author Contributions: Marc-Olivier Deguise: Generated the mouse model, designed study, produced and analyzed data for all figures, and wrote the manuscript. Yves De Repentigny: Data acquisition, data analysis and method description. Alexandra Tierney: Data acquisition and data analysis

Ariane Beauvais: Assistance with experiments. Jean Michaud: Assessment of histology of the skeletal muscle. Lucia Chehade: Data acquisition and data analysis. Mohamed Thabet: Assistance with electrophysiology. Brittany Paul: Data acquisition and data analysis. Aoife

Reilly: Assistance with experiments. Sabrina Gagnon: Maintenance of mouse models and genotyping. Jean-Marc Renaud: Electrophysiology and data analysis. Rashmi Kothary: Designed study and wrote manuscript.

Ileo-colonic delivery of conjugated bile acids improves glucose homeostasis via colonic GLP-1-producing enteroendocrine cells in human obesity and diabetes. (*EBioMedicine* **55:** 102,759)

Author Contributions: Conceptualization, AA, MC, FMG, and AV; Methodology, AM, AA, JR, BG, MC, FMG, and AV; Formal Analysis, GC, AM, JR, AA, FMG, and AV; Investigation, GC, AM, AA, JR, JD, IZ, GF, DB, GR, BG, SN, AA. Resources, FR, BG, AV, NFL, FMG, MC, AA. Writing – Original Draft: GC, AM, JR. Writing – Review & Editing, GC, AM, AA, JR, JD, GF, DB, GR, FR, BG, AV, NFL, FMG, MC, AA. Visualization, GC, AM, JR, Supervision FR, BG, AV, NFL, FMG, MC, AA Funding Acquisition, FMG, AA.

Longitudinal characteristics of lymphocyte responses and cytokine profiles in the peripheral blood of SARS-CoV-2 infected patients. (*EBioMedicine* **55:** 102,763)

Authors contributions: Conceptualization: JL, SML, JL, YH, DLY, XZ. Acquisition of data: BYL, XBW, HW, WL, QXT, JHY, LZ, LJX, CXG, JT, JZL, JHY, RP, HS, CP, TL, QZ, JW, LX, SHL, BJW, ZHW, CRH, HBZ, RZ, HLZ, XC, PY, BZ, LW,WQZ SSH,YWH, SHJ, PW, JAZ, YPL, WXW, LZ, LL, FQZ. Analysis and interpretation of data: JL, SML, JW. Writing-original draft Preparation: JL. Writing-review and editing: UD, MJL, JL, DLY, XZ. All authors reviewed and approved the final version of the manuscript.

A dysregulated bile acid-gut microbiota axis contributes to obesity susceptibility. (*EBioMedicine* **55:** 102,766)

Author contributions: Wei Jia was principal investigator of this study. Zhaoxiang Bian provided valuable support for C. scindens gavage animal experiment. Wei Jia, Aaihua Zhao, Xiaojiao Zheng, and Guoxiang Xie designed the study. Meilin Wei conducted key experiments of the study and perform the data analysis and drafted the manuscript. Fengjie Huang, Yunjing Zhang, Wei Yang, and Ling Zhao conducted the animal experiments. Kun Ge, Chun Qu, Mengci Li, Shouli Wang, and Xiaolong Han helped to perform the experiments and collected the data. Wei Jia and Cynthia Rajani revised the manuscript.

Prognostic and predictive value of a five-molecule panel in resected pancreatic ductal adenocarcinoma: A multicentre study. (*EBioMedicine* **55:** 102,767)

Author Contributions: Conception and design: JCG, SL, TPZ. Provision of study material and patients: JCG, SL, TPZ, ZGZ, BS, QL, MHD. Financial and administrative support: JCG, SL. Data analysis and interpretation: PZ, LZ, LY, QFL, ZYL, JL, DY, ADT, JS. Experimental support: PZ, LZ, LY, GGX. Manuscript writing: PZ, LZ, QFL. Final approval of the manuscript: All the authors.

CD24-targeted intraoperative fluorescence image-guided surgery leads to improved cytoreduction of ovarian cancer in a preclinical orthotopic surgical model. (*EBioMedicine* **56:** 102,783)

Author contributions: Literature search: E. McCormack, L. Bjørge, K. Kleinmanns, V. Fosse; Study design: E. McCormack, L. Bjørge, K. Kleinmanns, V. Fosse;

Development of methodology: E. McCormack, L. Bjørge, K. Kleinmanns, V. Fosse; Data collection (*in vitro* data, animal experiments, patient data): K. Kleinmanns, V. Fosse, B. Davidson, O. Tenstad, E. García de Jalón; Data analysis and interpretation of data (statistical analysis): K. Kleinmanns, V. Fosse, B. Davidson, O. Tenstad, E. García de Jalón; Writing, review and/or revision of the manuscript: K. Kleinmanns, V. Fosse, E. McCormack, L. Bjørge; Study supervision: E. McCormack, L. Bjørge. All authors read and approved the final version of the manuscript.

Low oxygen saturation during sleep reduces CD1D and RAB20 expressions that are reversed by CPAP therapy. (*EBioMedicine* **56:** 102,803)

Author contributions: TS, DJG, and SAG conceptualized the association study. TS, RL, RJ, HL, ACG, NK, BEC, JL, and SW performed statistical analysis and data harmonization. All authors critically reviewed the manuscript. YL, JR, and SR collected data and designed components of MESA and its gene expression study. DL collected data and designed components of FOS and the SABRe CVD initiative which collected genes expression data for FOS. RM, SRP, SFQ, SR, and DJG designed and executed the HeartBEAT study, and DJG and AS designed its gene expression study.

Clinical implications of serum neurofilament in newly diagnosed MS patients: A longitudinal multicentre cohort study. (*EBioMedicine* **56:** 102,807)

Author Contributions: FS, VF, TU, M Muthuraman, SGM, SG: Analysis and interpretation of data and drafting the manuscript. AS, RG: Study protocol, design and ethics implementation of the KKNMS cohort study. CL, AS, FL, TK, M Mühlau, LK, TR, A Bayas, A Berthele, FP, HPH, RL, CH, MS, BW, FTB, BT, TK, FW, UZ, UZ, HT, BH, HW, RG: Contributing data and revising the manuscript. SB, FZ: Design and conceptualisation of the study, analysis and interpretation of data, drafting the manuscript.

Molecular analysis of Chinese oesophageal squamous cell carcinoma identifies novel subtypes associated with distinct clinical outcomes. (*EBioMedicine* **57:** 102,831)

Author contributions: Lin Feng and Xiyan Wang designed the study. Meng Liu performed the data collection and data analysis. Wei Sun and Yuan Zhang collected Chinese ESCC samples. Haiyin An and Meng Liu extracted and quantified RNA and DNA. Shujun Cheng provided constructive feedback. Lin Feng and Ruozheng Wang supervised research and provided data interpretation. Meng Liu wrote and reviewed the manuscript.

Using Recombination-Dependent Lethal Mutations to Stabilize Reporter Flaviviruses for Rapid Serodiagnosis and Drug Discovery. (*EBioMedicine* **57:** 102,838)

Author contributions: C.B., X.X, and A.M. performed experiments. K.F. provided critical reagents. C.B., X.X., J.Z., and A.M. analyzed the data. C.B., X.X., J.Z., K.F., and P-Y.S. interpreted results. C.B., X.X., and P-Y.S. wrote the manuscript.

Broadly neutralizing antibodies potently inhibit cell-to-cell transmission of semen leukocyte-derived SHIV162P3. (*EBioMedicine* **57:** 102,842)

Author contributions: Study conception and design: RLG and MC. Acquisition of data: KS, MT, and SH. Management of animals: DD. VL, HM and GS contributed with key reagents and expertise. Analysis and interpretation of the data: KS, NDB, and MC. Draft of the manuscript: KS and MC. Critical revisions: HM, GS, RLG, and MC. All authors read and approved the final version of the manuscript.

GSTM3 variant is a novel genetic modifier in Brugada syndrome, a disease with risk of sudden cardiac death. (*EBioMedicine* **57:** 102,843)

Author Contributions: JMJJ, TPL, and CA performed literature search, conceived and designed the study and the experiments. JMJJ, TPL, AB, IR, SJL, CYJC, LCL, SFSY, EYC, and LPL conducted experiments and analysed the data. JMJJ, JJH, WCC, YBL, LYL, CCY, LTH, and HCH enrolled patients, collected and interpreted data. JMJJ, AB, IR, TPL, and CA wrote the paper.

Tumor budding, poorly differentiated clusters, and T-cell response in colorectal cancer. (*EBioMedicine* **57:** 102,860)

Author contributions: All authors contributed to review and revision. M.G., J.A.N., and S.O.: developed the main concept and designed the study. A.T.C., C.S.F., M.G., and S.O.: wrote grant applications. K.F., J.P.V., J.B., D.J.P., J.A.M., A.T.C., C.S.F., J.K.L., J.A.N., and S.O.: were responsible for collection of tumor tissue, and acquisition of epidemiologic, clinical and tumor tissue data, including histopathological, immunohistochemical, and immunofluorescent characteristics. K.F., J.P.V., J.B., D.J.P., K.H., J.A.M., C.S.F., J.A.N., and S.O.: performed data analysis and interpretation. K.F., J.P.V., J.B., D.J.P., and S.O.:

drafted the manuscript. K.A., K.H., J.K., N.A., T.U., M.C.L., S.G., S.S., M.Z., A.F.L.D.S., T.S.T, H.N., J.A.M., X.Z., K.W., M.G., J.A.N., and S.O.: contributed to editing and critical revision for important intellectual contents.

A surrogate of Roux-en-Y gastric bypass (the enterogastro anastomosis surgery) regulates multiple beta-cell pathways during resolution of diabetes in ob/ob mice. (*EBioMedicine* **58:** 102,895)

Author contributions: F.A., C.A. and C.M. designed the experiments. C.A.; J.C.; C.G.; A.L.; F.M., C.R., J.D.; E.G.; S.M.L., O.T. conducted the experiments. C.A.; F.A.; C.M.; O.T.; C.G. G.R. and R.R. analyzed data. K.C. contributed to patient recruitment and coordinated clinical investigation, patient phenotyping, and sample collection. F.A. and C. A. wrote the manuscript and C.A.; F.A.; C.M.; O.T.; T.S.; C.G.; R.R.; S.L.; R.S.; H.L.S.; E.G. and G.R. contributed to data presentation and the manuscript. All authors reviewed the manuscript. F.A. is the guarantor of this work and, as such, had full access to all the data in the study and takes responsibility for the integrity of the data and the accuracy of the data analysis.

Protection Against Mycobacterial Infection: a case-control study of mycobacterial immune responses in pairs of Gambian children with discordant infection status despite matched TB exposure. (*EBioMedicine* **59:** 102,891)

Author contributions: RB and BK conceived and designed the work. RB, MS, AS and UE conducted the clinical recruitment. RB and BS conducted and interpreted the BCG-GFP-LuxFO whole blood assays. BS and MG conducted the in-house interferon gamma release assays. BH conducted and interpreted the cytokine multiplex assays. RB and AK conducted the statistical analyses. RB and BK drafted the work. All authors revised the work for important intellectual content.

Brain Delivery of Supplemental Docosahexaenoic Acid (DHA): A Randomized Placebo-Controlled Clinical Trial. (*EBioMedicine* **59:** 102,883)

Author contributions: IC, NC, BK, DB participated in recruitment and study visits. HNY and MGH did lumbar punctures. XH, NK, and WJM conducted data analysis. NH, NK and MNB did imaging analysis. LD, CM, and HCC planned cognitive testing. AM, AS, BZ assisted with biomarkers. IC, VS, HH, MH, HCC, WJM, MNB, LSS and HNY wrote the manuscript. HNY and LSS designed the study.

Obesity-related hypoxia via miR-128 decreases insulin-receptor expression in human and mouse adipose tissue promoting systemic insulin resistance. (*EBioMedicine* **59:** 102,912)

Author contributions: B.A. and F.L.A. performed experiments *in vitro* and *in vivo*, in mouse systems; B.A. performed human tissue culture studies and analyzed data with the contribution of E.C., M.M., D. M.C., D.P.F and A.B; G.C. and G.N. provided tissues from surgery and clinical information; D.B., V.M. and UK contributed to the analysis of data from mouse experiments; B.A. and E.C. contributed to manuscript draft; F.S.B. helped collecting clinical data and drafted figures; I. D.G. edited the final version of the manuscript and contributed to data interpretation; A.B. conceived and supervised the study and wrote the manuscript.

All authors read and approved the final manuscript.